CellPress
Partner Journal

Molecular Plant
Research article

OsPRMT6a-mediated arginine methylation of OsJAZ1 regulates jasmonate signaling and spikelet development in rice

Kun Dong[1,3], Fuqing Wu[1,3], Siqi Cheng[2,3], Shuai Li[1], Feng Zhang[1], Xinxin Xing[1], Xin Jin[1], Sheng Luo[1], Miao Feng[1], Rong Miao[2], Yanqi Chang[1], Shuang Zhang[1], Xiaoman You[2], Peiran Wang[2], Xin Zhang[1], Cailin Lei[1], Yulong Ren[1], Shanshan Zhu[1], Xiuping Guo[1], Chuanyin Wu[1], Dong-Lei Yang[2], Qibing Lin[1,*], Zhijun Cheng[1,*] and Jianmin Wan[1,2,*]

[1]State Key Laboratory of Crop Gene Resources and Breeding, National Key Facility for Crop Gene Resources and Genetic Improvement, Institute of Crop Sciences, Chinese Academy of Agricultural Sciences, Beijing 100081, China

[2]State Key Laboratory for Crop Genetics and Germplasm Enhancement, Nanjing Agricultural University, Nanjing 210095, China

[3]These authors contributed equally to this article.

***Correspondence: Qibing Lin (linqibing@caas.cn), Zhijun Cheng (chengzhijun@caas.cn), Jianmin Wan (wanjianmin@caas.cn)**

https://doi.org/10.1016/j.molp.2024.04.014

ABSTRACT

Although both protein arginine methylation (PRMT) and jasmonate (JA) signaling are crucial for regulating plant development, the relationship between these processes in the control of spikelet development remains unclear. In this study, we used the CRISPR/Cas9 technology to generate two *OsPRMT6a* loss-of-function mutants that exhibit various abnormal spikelet structures. Interestingly, we found that OsPRMT6a can methylate arginine residues in JA signal repressors OsJAZ1 and OsJAZ7. We showed that arginine methylation of OsJAZ1 enhances the binding affinity of OsJAZ1 with the JA receptors OsCOI1a and OsCOI1b in the presence of JAs, thereby promoting the ubiquitination of OsJAZ1 by the $SCF^{OsCOI1a/OsCOI1b}$ complex and degradation via the 26S proteasome. This process ultimately releases OsMYC2, a core transcriptional regulator in the JA signaling pathway, to activate or repress JA-responsive genes, thereby maintaining normal plant (spikelet) development. However, in the *osprmt6a-1* mutant, reduced arginine methylation of OsJAZ1 impaires the interaction between OsJAZ1 and OsCOI1a/OsCOI1b in the presence of JAs. As a result, OsJAZ1 proteins become more stable, repressing JA responses, thus causing the formation of abnormal spikelet structures. Moreover, we discovered that JA signaling reduces the *OsPRMT6a* mRNA level in an OsMYC2-dependent manner, thereby establishing a negative feedback loop to balance JA signaling. We further found that OsPRMT6a-mediated arginine methylation of OsJAZ1 likely serves as a switch to tune JA signaling to maintain normal spikelet development under harsh environmental conditions such as high temperatures. Collectively, our study establishes a direct molecular link between arginine methylation and JA signaling in rice.

Key words: protein arginine methylation, jasmonate signaling, negative feedback loop, spikelet development, adaptation to heat stress, rice

Dong K., Wu F., Cheng S., Li S., Zhang F., Xing X., Jin X., Luo S., Feng M., Miao R., Chang Y., Zhang S., You X., Wang P., Zhang X., Lei C., Ren Y., Zhu S., Guo X., Wu C., Yang D.-L., Lin Q., Cheng Z., and Wan J. (2024). OsPRMT6a-mediated arginine methylation of OsJAZ1 regulates jasmonate signaling and spikelet development in rice. Mol. Plant. **17**, 900–919.

INTRODUCTION

Jasmonates (JAs), comprising jasmonic acid and its volatile ester derivative methyl-jasmonate (MeJA) and amino acid derivatives (such as jasmonyl-isoleucine [JA-Ile]), are important phytohormones that not only mediate plant defense responses to pathogens, herbivores, and abiotic stresses but also regulate plant growth and developmental processes such as sexual

Published by the Molecular Plant Shanghai Editorial Office in association with Cell Press, an imprint of Elsevier Inc., on behalf of CSPB and CEMPS, CAS.

reproduction, root elongation, carbohydrate accumulation, floret development, and fruit ripening (Browse and Howe, 2008; Pauwels et al., 2008; Acosta et al., 2009; Chung and Howe, 2009; Kim et al., 2009; Yoshida et al., 2009b; Lee et al., 2013; Hori et al., 2014; Goossens et al., 2017; Huang et al., 2017; Guo et al., 2018; Chico et al., 2020; Hu et al., 2023). The JA biosynthesis and signaling pathways in rice (*Oryza sativa* L.) and *Arabidopsis thaliana* (*Arabidopsis*) have been well established. In JA signaling in *Arabidopsis* and rice, the JA receptors Coronatine-Insensitive 1 (COI1) and OsCOI1a/OsCOI1b are F-box proteins that bind to S-phase kinase-associated protein 1 (Skp1), Cullin, and Rbx1 proteins to form the SCF^{COI1} E3 ubiquitin ligase complex (Devoto et al., 2002; Xu et al., 2002; Yang et al., 2012). The jasmonate ZIM domain (JAZ) proteins (comprising 12 members) and OsJAZs (comprising 15 members, OsJAZ1 to OsJAZ15) belong to the plant-specific TIFY family and function as repressors of the JA signaling pathway (Chini et al., 2007; Thines et al., 2007; Ye et al., 2009). The basic-helix-loop-helix transcription factor MYC2 and its homolog OsMYC2 are master regulators of most aspects of the JA signaling pathway. In the absence of JAs, JAZs/OsJAZs bind to MYC2/OsMYC2 to inhibit JA responses (Dombrecht et al., 2007; Cai et al., 2014). However, in the presence of JAs, JAZs/OsJAZs bind to the receptors COI1/OsCOI1a/OsCOI1b, promoting binding of the $SCF^{COI1/OsCOI1a/OsCOI1b}$ complex to JAZs/OsJAZs for ubiquitination, after which the ubiquitinated JAZs/OsJAZs are degraded by the 26S proteasome (Xu et al., 2002; Ye et al., 2009; Sheard et al., 2010; Yamada et al., 2012; Cai et al., 2014; Wu et al., 2015; Feng et al., 2020; He et al., 2020; Cao et al., 2021), thereby releasing MYC2/OsMYC2 to activate or repress downstream JA-responsive genes (Chung and Howe, 2009). The genes activated by MYC2 include *VEGETATIVE STORAGE PROTEIN* (*VSP*) and *LIPOXYGENASE 3* (*LOX3*), which are involved in the injury response in *Arabidopsis*, and the genes activated by OsMYC2 include spikelet development-related genes such as *OsMADS1*, *OsMADS7*, and *OsMADS14* in rice. The genes repressed by MYC2 include *PATHOGENESIS-RELATED 1* (*PR1*), the defense gene *PLANT DEFENSIN 1.2* (*PDF1.2*), the stress-related gene *CHITINASE B* (*CHIB*), and *PATHOGENESIS-RELATED 4* (*PR4*) (Reymond et al., 2000; Cheong et al., 2002; Brown et al., 2003; Lorenzo et al., 2004; Chen et al., 2006; You et al., 2019).

The spikelet is the fundamental unit of inflorescence structure in grasses, consisting of rudimentary glumes and sterile lemmas, as well as a single fertile floret comprising a lemma, a palea, two lodicules, six stamens, and one pistil (Yoshida and Nagato, 2011). Spikelet development is crucial for the formation of inflorescence structure and grain yield. Many genes that control rice spikelet development, such as *LONG STERILE LEMMA* (*ELE*, *G1*), *MULTI-FLORET SPIKELET 1* (*MFS1*), *INDETERMINATE SPIKELET 1* (*OsIDS1*), *OsMADS1*, *OsMADS7*, and *OsMADS14*, have been identified (Jeon et al., 2000; Lim et al., 2000; Komatsu et al., 2003; Malcomber and Kellogg, 2004; Chen et al., 2006; Lee et al., 2007; Yoshida et al., 2009a; Cui et al., 2010; Lee and An, 2012; Ren et al., 2013; Zhang et al., 2017). In addition to regulating defense responses, JA signaling also regulates spikelet development in plants. For instance, abnormal spikelet morphology has been observed in mutants with loss of function of genes related to JA synthesis, such as *EXTRA GLUME1* (*EG1*) and *PEROXIN 5* (*OsPEX5*) (Lim et al., 2000; Li et al., 2009; Cui et al., 2010; You et al., 2019). In addition, abnormal spikelet development has been observed upon ectopic expression of the OsJAZ JA-signaling repressors (Cai et al., 2014; Hori et al., 2014; Cao et al., 2021). Notably, JA signaling can shape spikelet morphology through OsMYC2-mediated regulation of *OsMADS1*, *OsMADS7*, and *OsMADS14* (Chen et al., 2006; You et al., 2019).

Protein arginine methylation is a common and significant post-translational modification in eukaryotes that plays a crucial role in various biological processes, including transcriptional regulation, chromatin remodeling, RNA metabolism, protein nucleocytoplasmic translocation, signal transduction, and apoptosis (Bedford and Clarke, 2009; Blanc and Richard, 2017). Protein arginine methylation is catalyzed by a family of enzymes known as protein arginine methyltransferases (PRMTs) that methylate histones and a wide array of nonhistone proteins (Bedford and Clarke, 2009). PRMTs facilitate the transfer of methyl groups from *S*-adenosyl-L-methionine to arginine residues within target proteins. Depending on the position and number of methyl groups attached to the ω-guanidine nitrogen atom of arginine, methylated arginine can be categorized into three types: monomethylarginine, symmetric dimethylarginine, and asymmetric dimethylarginine (Wolf, 2009).

PRMTs are widely distributed in single-celled organisms, eukaryotic yeasts, higher animals, and plants. Humans harbor 11 members of the PRMT family, PRMT1 to PRMT11. All possess conserved catalytic functional domains, including motifs I, post-I, -II, and -III, the "double E motif," and the THW (Thr-His-Trp) loop (Cheng et al., 2005). Most research on arginine methyltransferases in higher plants has been carried out in *Arabidopsis*, with only limited studies in rice. *A. thaliana* contains nine homologous PRMT proteins. Among these, AtPRMT1a and AtPRMT1b, which are homologs of human PRMT1, synergistically and asymmetrically dimethylate histone H4, H2A, myelin basic protein, and AtFib2 (Yan et al., 2007). Research *in planta* has shown that AtPRMT3 deficiency results in an imbalance and abnormalities in the pre-rRNA processing pathway (Hang et al., 2014). AtPRMT4a, AtPRMT4b, AtPRMT5, AtPRMT10, and AtPRMT11 participate in flowering regulation in *Arabidopsis* (Pei et al., 2007; Wang et al., 2007; Schmitz et al., 2008; Hong et al., 2010), and an *atprmt11* mutant exhibited abnormal inflorescence morphology with several sterile florets (Scebba et al., 2007). *O. sativa* has eight homologous PRMT proteins, OsPRMT1, OsPRMT3, OsPRMT4, OsPRMT5, OsPRMT6a, OsPRMT6b, OsPRMT7, and OsPRMT10, and although their methylation activities have been confirmed *in vitro*, their specific substrates and biological functions *in planta* are still poorly understood (Ahmad et al., 2011). In particular, the biological functions of AtPRMT6 in *Arabidopsis* and OsPRMT6a and OsPRMT6b in rice remain unclear.

Here, we found that loss of OsPRMT6a function leads to abnormal spikelet morphology. OsPRMT6a methylates the arginine residues of OsJAZ1. Arginine-methylated OsJAZ1 has a stronger affinity for OsCOI1a/OsCOI1b, thus facilitating the ubiquitination of OsJAZ1 by the $SCF^{OsCOI1a/OsCOI1b}$ complex and the subsequent degradation of ubiquitinated OsJAZ1 by the 26S proteasome. This mechanism enables the effective transmission of JA signaling, which is crucial for proper spikelet development.

In addition, MeJA downregulates the mRNA level of *OsPRMT6a* through OsMYC2 via a negative feedback loop. Thus, our study establishes a direct link between protein arginine methylation and JA signaling, a relationship critical for rice spikelet development.

RESULTS

Mutation in *OsPRMT6a* causes abnormal spikelet morphology

To characterize the developmental biology of rice spikelets, we used CRISPR/Cas9 technology to construct a mutant library from which two mutants with abnormal spikelet morphology were isolated. Sequencing analysis revealed a 1-bp deletion in *osprmt6a-1* and a 1-bp insertion in *osprmt6a-2* within the *OsPRMT6a* (Os10g0489100) gene (Figure 1A). Compared with the wild type (WT), both mutants exhibited various abnormal spikelet structures, ranging from nearly normal structures to those with extreme deformities, including long sterile lemma, long sterile lemma and spikelet-like structures, eight stamens, three stigmas and stamen-like organs, and other deviations (Figure 1B–1U and Supplemental Table 1). Scanning electron micrographs of spikelets at early stages Sp 5 to Sp 6 in *osprmt6a-1* revealed bulging floral meristems, abnormal sterile lemma, ectopic stamen-like structures, and irregular glume-like structures (Supplemental Figure 1). In addition, the two mutants exhibited atypical agronomic traits, such as shorter plant height, increased tiller number, lower seed-setting rate, and altered panicle type and grain size (Supplemental Figure 2).

To confirm that the *OsPRMT6a* mutation caused these phenotypes, we performed RNA interference (RNAi) analysis and a transgenic complementation test. The results showed that the phenotypes of the *OsPRMT6a*-RNAi lines (Ri1 and Ri2) mirrored those of *osprmt6a-1* and *osprmt6a-2*, and those of the transgenic complementation line resembled those of the WT (Supplemental Figure 3), confirming that the *osprmt6a-1* and *osprmt6a-2* mutant phenotypes were caused by mutations in *OsPRMT6a*. Given the similar phenotypes of *osprmt6a-1* and *osprmt6a-2*, we used *osprmt6a-1* exclusively in subsequent experiments.

Phylogenetic and protein sequence analyses revealed that OsPRMT6a is a typical protein arginine methyltransferase with conserved PRMT signature motifs I, post-I, -II, and -III, a THW loop (black bars), and a double E loop (Supplemental Figures 4 and 5). RT–qPCR analysis revealed widespread expression of *OsPRMT6a*, with relatively high levels in leaf sheaths and panicles (Supplemental Figure 6A). Subcellular localization analysis of rice protoplasts revealed a predominantly nuclear localization with a weak membrane distribution (Supplemental Figure 6B and 6C). mRNA *in situ* hybridization revealed that *OsPRMT6a* was widely expressed in the inflorescence meristem, primary branch meristem, secondary branch meristem, and spikelet (Supplemental Figure 6D–6H).

In conclusion, these results suggest that OsPRMT6a likely participates in the regulation of various plant development processes, including spikelet development.

OsPRMT6a physically interacts with several OsJAZs and methylates arginine residues in OsJAZ1

To explore how OsPRMT6a regulates spikelet development, we performed yeast two-hybrid (Y2H) library screening to identify potential substrates of OsPRMT6a. Because the abnormal spikelet morphology in *osprmt6a* closely resembles that caused by mutations in JAZ family proteins (Cai et al., 2014; Hori et al., 2014), we selected JAZ family proteins identified from the Y2H library screening as candidate OsPRMT6a substrates for use in subsequent experiments.

To investigate the interaction between OsPRMT6a and 15 members of the rice JAZ family, we performed Y2H assays and revealed that OsJAZ5, OsJAZ6, OsJAZ7, and OsJAZ8 physically interact with OsPRMT6a (Supplemental Figure 7). Subsequently, through *in vivo* coimmunoprecipitation (Co-IP), *in vitro* pull-down, luciferase (LUC) complementation imaging, and bimolecular fluorescence complementation (BiFC) assays, we confirmed that OsPRMT6a interacts with OsJAZ1, OsJAZ7, and OsJAZ8 (Figure 2A–2D and Supplemental Figure 8).

The protein interaction analysis results suggested that some OsJAZs (OsJAZ1, OsJAZ7, and OsJAZ8) were potential OsPRMT6a substrates. To verify this, OsJAZ1 was selected as a representative protein for use in subsequent analyses because of its well-defined role in JA signaling. An *in vitro* methylation assay showed that OsJAZ1 was methylated by OsPRMT6a (Figure 2E). We then used methylated OsJAZ1 obtained from an *in vitro* methylation assay to analyze the specific methylation sites catalyzed by OsPRMT6a via mass spectrometry and ultimately identified five distinct arginine methylation sites (Figure 2G–2I). Furthermore, using mass spectrometry, we analyzed the methylation of OsJAZ1-green fluorescent protein (GFP) proteins immunoprecipitated with an anti-GFP antibody from transgenic plants in the WT and *osprmt6a-1* backgrounds. An arginine modification site was found only in OsJAZ1-GFP from the WT, not in those from *osprmt6a-1* background transgenic plants (Supplemental Figure 9), suggesting that OsJAZ1 is likely methylated *in vivo* by OsPRMT6a. Using the same method, we also identified two arginine methylation sites in OsJAZ7 that were modified *in vitro* by OsPRMT6a (Supplemental Figure 10).

To validate the five arginine methylation sites in OsJAZ1, we substituted them with lysine to prevent methylation. The replacement of the 58th amino acid (an arginine methylation site identified by *in vivo* immunoprecipitation–mass spectrometry) with one lysine is represented as "1K," and "5K" denotes the replacement of all five identified arginines with lysines in OsJAZ1, mimicking the nonmethylated state of the protein. An *in vitro* arginine methylation assay confirmed that OsJAZ1 (5K) had less methylation catalyzed by OsPRMT6a than did OsJAZ1 and OsJAZ1 (1K) (Figure 2E), confirming that the five arginines were indeed the sites of OsJAZ1 methylation catalyzed by OsPRMT6a.

To investigate whether OsPRMT6a methylates OsJAZ1 *in vivo*, we generated *p35S*:*OsJAZ1-GFP*/WT (in the WT background) and *p35S*:*OsJAZ1-GFP*/*osprmt6a-1* (in the *osprmt6a-1* background) transgenic lines. Lines with similar *OsJAZ1* expression levels (L4-8 and L3-1) were used for subsequent experiments

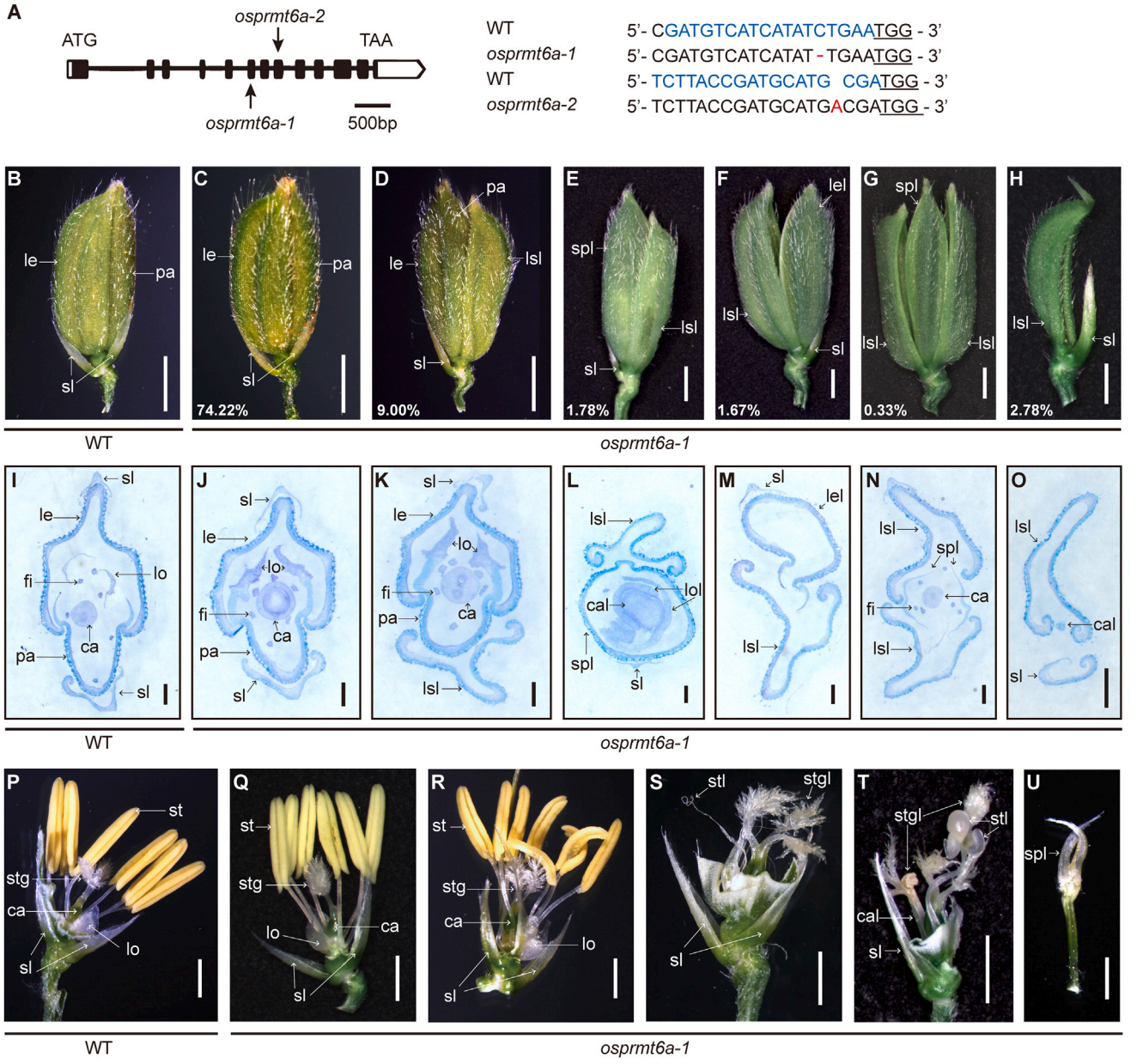

Figure 1. Abnormal spikelet development of the *osprmt6a-1* mutant.

(A) Targeted mutation of *OsPRMT6a* by CRISPR/Cas9 technology. The diagram shows the genomic structure of *OsPRMT6a*. Arrows indicate target sites. Exons, introns, and untranslated regions are denoted by black boxes, lines, and white boxes, respectively. The right panel displays the sequence alignment of WT, *osprmt6a-1*, and *osprmt6a-2*, highlighting the CRISPR/Cas9-induced mutated sites. Blue font shows the 18-bp CRISPR/Cas9 target sequences adjacent to the underlined protospacer adjacent motifs.

(B–H) Spikelet morphology, including normal spikelets in the WT **(B)** and various spikelet morphologies in *osprmt6a-1*: normal spikelet **(C)** and abnormal spikelets with long sterile lemma **(D)**, long sterile lemma and spikelet-like structure **(E)**, long sterile lemma and lemma-like structure **(F)**, two long sterile lemmas and spikelet-like structure **(G)**, and one separate long sterile lemma and one sterile lemma **(H)**. The ratio of the specific mutation type (2020, Shunyi district, Beijing) is marked in the lower left corner.

(**I–O)** Transverse resin semi-thin sections from **(B)–(H)**.

(P) WT floret with six stamens, two lodicules, one carpel, and two stigmas. The lemma and palea were removed.

(Q–U) *osprmt6a-1* produces normal florets like those of the WT **(Q)** and abnormal florets with eight stamens **(R)**, three stigmas and a stamen-like organ **(S)**, severely malformed carpel, stamen, and stigma **(T)**, and a degenerated spikelet **(U)**.

le, lemma; lel, lemma-like structure; pa, palea; sl, sterile lemma; st, stamen; lo, lodicule; fi, filament; stg, stigma; stgl, stigma-like structure; lsl, long sterile lemma; spl, spikelet-like structure; ca, carpel; cal, carpel-like structure; stl, stamen-like structure. Scale bars, 2 mm **(B–H)**, 500 μm **(I–O)**, and 1 mm **(P–U)**.

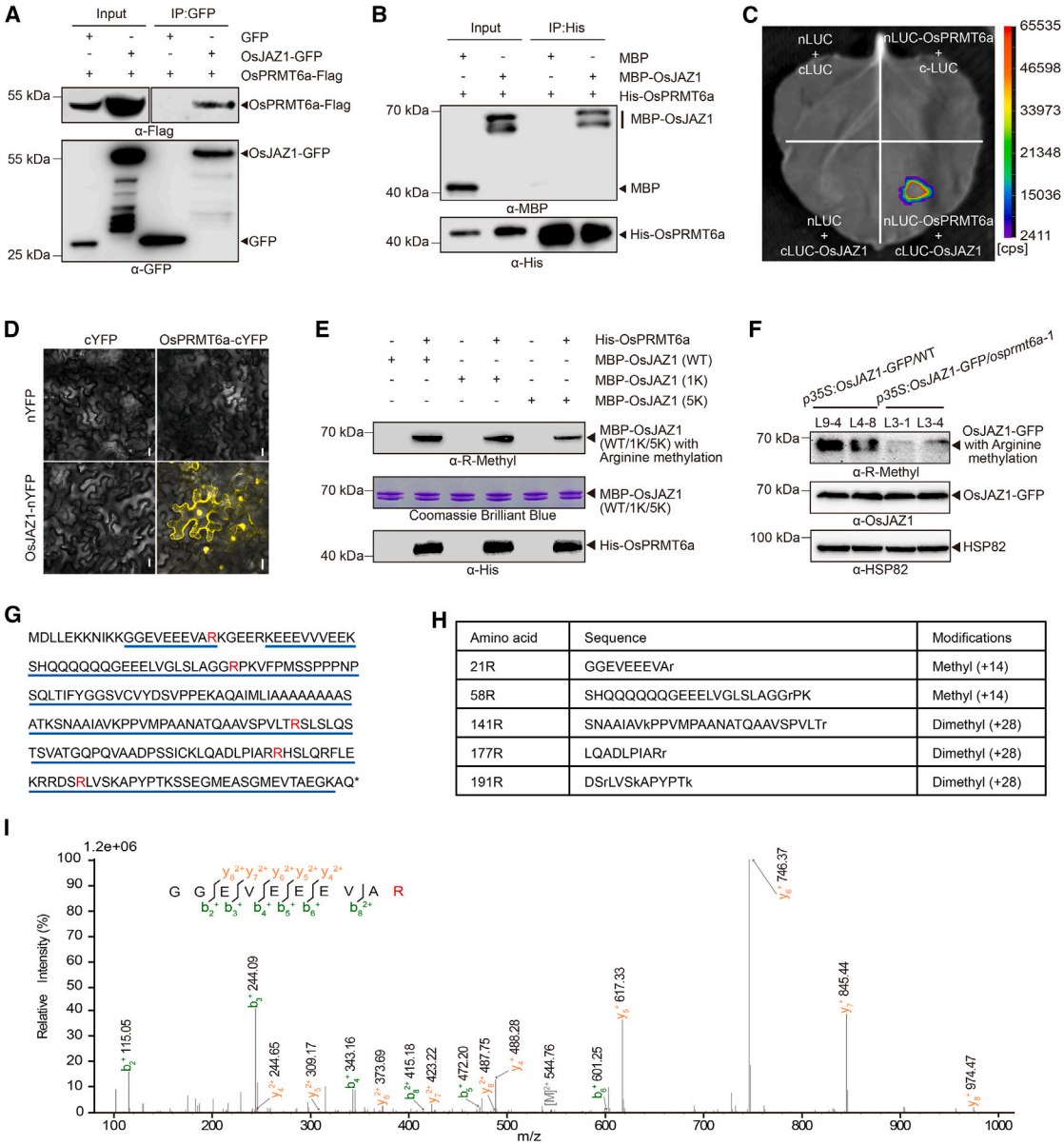

Figure 2. OsPRMT6a physically interacts with OsJAZ1 to methylate its arginine residues.

(A) *In vivo* coimmunoprecipitation (Co-IP) assay showing the interaction between OsPRMT6a and OsJAZ1 in *N. benthamiana* leaves. The molecular weights (MWs) of OsJAZ1 and GFP are 23.02 kDa and 27.12 kDa, respectively. The theoretical MW of the OsJAZ1-GFP fusion protein, including the linking residue, is 51.28 kDa. Owing to post-translational modifications such as arginine methylation and ubiquitination, the observed band for OsJAZ1-GFP appears slightly higher than the 55-kDa band of the MW marker.

(B) *In vitro* pull-down assay showing the interaction of OsPRMT6a with OsJAZ1. His-OsPRMT6a proteins were incubated with MBP-OsJAZ1 or MBP proteins. Protein samples were immunoprecipitated with anti-His antibodies and immunoblotted with anti-His and anti-MBP antibodies.

(C) Luciferase complementation imaging (LCI) assay showing the interaction of OsPRMT6a with OsJAZ1 in *N. benthamiana* leaves. The pseudocolor bar (right panel) shows the range of luminescence intensity in each image.

(D) Bimolecular fluorescence complementation (BiFC) assay showing the interaction between OsPRMT6a and OsJAZ1 in leaf epidermal cells of *N. benthamiana*.

(E) OsPRMT6a methylates arginine residues of OsJAZ1 *in vitro*. Top and bottom panels: western blots; middle panel: Coomassie brilliant blue staining. OsJAZ1 (WT/1K/5K) represent WT OsJAZ1, OsJAZ1 with one arginine replaced by lysine, and OsJAZ1 with five arginines replaced by lysine, respectively.

(F) OsPRMT6a methylates arginine residues of OsJAZ1 *in vivo*. α-HSP82 shows an equal amount of total proteins, α-OsJAZ1 shows an equal amount of OsJAZ1-GFP protein in the total proteins, and α-R (arginine)-methyl shows the levels of methylated arginine residues in OsJAZ1-GFP proteins in plants.

(G) OsJAZ1 protein sequence showing methylated arginine residues (indicated with red font) *in vitro* by mass spectrometry analysis. The blue underlined residues represent the coverage extent of the identified protein peptides.

(H) Table listing methylated peptides and their methylation modification status detected by mass spectrometry.

(I) Representative mass spectrometry result showing a methylated arginine residue in the GGEVEEEVAR peptide of the OsJAZ1 protein.

The symbols "−" and "+" denote the absence and presence of the corresponding proteins. Scale bars, 20 μm.

(Supplemental Figure 11). OsJAZ1-GFP overexpression did not affect the phenotype of the recipient plants. Notably, the *p35S*:*OsJAZ1-GFP*/*osprmt6a-1* transgenic plants exhibited abnormal spikelet morphology similar to that of *osprmt6a-1*, whereas *p35S*:*OsJAZ1-GFP*/WT transgenic plants displayed normal spikelet morphology similar to that of the WT plants (Supplemental Figure 12). Detection of OsJAZ1-GFP with an anti-arginine methylation antibody revealed higher arginine methylation levels of OsJAZ1-GFP in the WT plants than in the *osprmt6a-1* plants (Figure 2F). According to the developmental stages of rice spikelets defined in previous research (Ikeda et al., 2004), we assessed the OsJAZ1-GFP level and OsJAZ1-GFP arginine methylation levels in rice spikelets from stages In 3 to In 9. The OsJAZ1-GFP level increased, whereas the OsJAZ1-GFP arginine methylation level decreased, from stages In 3 to In 6. The lowest OsJAZ1-GFP level, accompanied by the highest arginine methylation level, occurred at stage In 7, and there was a return to lower OsJAZ1-GFP levels with reduced arginine methylation levels from stages In 8 to In 9 (Supplemental Figure 13). According to previous research (Ikeda et al., 2004), In 6 and In 7 are two key stages in the initiation and development of spikelet organs such as the sterile lemma, lemma, palea and various floret organs such as the stamen, lodicule, and carpel. Here, we observed severe downregulation of OsJAZ1-GFP content and strong upregulation of arginine methylation in OsJAZ1-GFP between the In 6 and In 7 stages (Supplemental Figure 13), which was consistent with the abnormal spikelets and floret organs observed in the *osprmt6a* mutants.

In summary, these results demonstrate that OsJAZ1 is methylated by OsPRMT6a both *in vivo* and *in vitro*, suggesting that OsPRMT6a likely regulates spikelet development by methylating OsJAZ1.

Arginine methylation of OsJAZ1 promotes its degradation

JAZs are known to serve as direct targets for the SCF^{COI1} E3 ubiquitin ligase, and the application of JAs induces the ubiquitination and degradation of JAZs (Xu et al., 2002; Chini et al., 2007). To investigate whether arginine methylation of OsJAZ1 influences JA-induced OsJAZ1 degradation, we subjected various rice seedlings to short-term treatment with different concentrations of MeJA. The results showed that both native OsJAZ1 protein and JAZ1-GFP fusion protein in the *osprmt6a-1* mutant background were less susceptible to degradation than those in the WT background under MeJA treatment (Figure 3A and 3B; Supplemental Figures 14 and 15).

Measurements of JA content revealed that the WT and *osprmt6a-1* seedlings had much lower JA contents than did their spikelets, and the WT had slightly lower JA content than the *osprmt6a-1* mutant (Figure 3C). Notably, the lower JA content in the seedlings likely led to less JA-induced degradation of OsJAZ1 and OsJAZ1-GFP, establishing a positive correlation between OsJAZ1/OsJAZ1-GFP levels and their mRNA levels in both the WT and *osprmt6a-1* backgrounds (Figure 3A–3E). However, in the spikelets, a greater JA content triggered substantial degradation of OsJAZ1 and OsJAZ1-GFP in the WT background but not in the *osprmt6a-1* background. This reduced the OsJAZ1 and OsJAZ1-GFP levels in the WT background compared with those in the *osprmt6a-1* background, despite the higher *OsJAZ1* mRNA levels in the WT background than in the *osprmt6a-1* background (Figure 3D and 3E).

To assess the effect of the modification status of the five identified arginine methylation sites on protein stability, we performed a dual-LUC degradation assay to compare the stabilities of the OsJAZ1 (5K) and OsJAZ1 proteins. Plasmids expressing the OsJAZ1 (5K)-LUC and OsJAZ1-LUC fusion proteins were constructed and transfected into *Nicotiana benthamiana* leaves. The LUC/REN bioluminescence ratio was measured at 48 h and 72 h post transfection. We observed accumulation of OsJAZ1 (5K) in the demethylated state, in contrast to decreasing amounts of OsJAZ1 over time (Figure 3F and 3G). Similarly, in a cell-free degradation assay, maltose-binding protein (MBP)-OsJAZ1 (5K) exhibited greater stability than MBP-OsJAZ1 over time (Figure 3H).

In conclusion, these results demonstrate that arginine methylation of OsJAZ1 by OsPRMT6a promotes OsJAZ1 degradation in rice.

Arginine methylation of OsJAZ1 promotes its interaction with OsCOI1a or OsCOI1b to facilitate OsJAZ1 ubiquitination

JAZs are known to bind to the JA receptor COI1 in the SCF^{COI1} complex, leading to the ubiquitination and subsequent degradation of the JAZs (Xu et al., 2002). In rice, OsCOI1a and OsCOI1b, which are homologs of COI1, function as receptors for JAs (Yang et al., 2012). To investigate whether arginine methylation of OsJAZ1 influences OsJAZ1 degradation by affecting the interaction of OsJAZ1 with OsCOI1a and OsCOI1b, we performed the following analyses.

The interaction between COI1 and JAZ is dependent on JA (Katsir et al., 2008; Sheard et al., 2010). We performed Y2H assays with coronatine (COR), a mimic of JA-Ile, in quadruple dropout medium as described previously (Cai et al., 2014). The results revealed an interaction between OsJAZ1 and OsCOI1b in the presence of COR, but no interaction was detected between OsJAZ1 and OsCOI1a (Figure 4A). We next performed semi-*in vivo and in vivo Co-IP assays* using *p35S*:*OsJAZ1-GFP*/WT and *p35S*:*OsJAZ1-GFP*/*osprmt6a-1* transgenic plants, along with the MBP-tagged fusion protein MBP-OsCOI1b (because we lacked an anti-OsCOI1b antibody) expressed in a prokaryotic system. OsJAZ1-GFP increased the enrichment of recombinant MBP-OsCOI1b proteins and native OsCOI1a proteins in total protein extracts from the *p35S*:*OsJAZ1-GFP*/WT transgenic plants compared with those from the *p35S*:*OsJAZ1-GFP*/*osprmt6a-1* transgenic plants (Figure 4B and 4C). Using a transient expression system in rice protoplasts for *in vivo* Co-IP assays, we detected stronger interactions of OsCOI1a-FLAG or OsCOI1b-FLAG with OsJAZ1-GFP than with the OsJAZ1 (5K)-GFP fusion protein (Figure 4D and 4E). This finding was inconsistent with previous reports that OsJAZ1 and OsCOI1a did not interact in BiFC and Y2H analyses (Cai et al., 2014; Cao et al., 2021). To determine the possible reasons for this inconsistency, we performed additional BiFC and luciferase complementation imaging (LCI) assays. Neither the LCI nor the

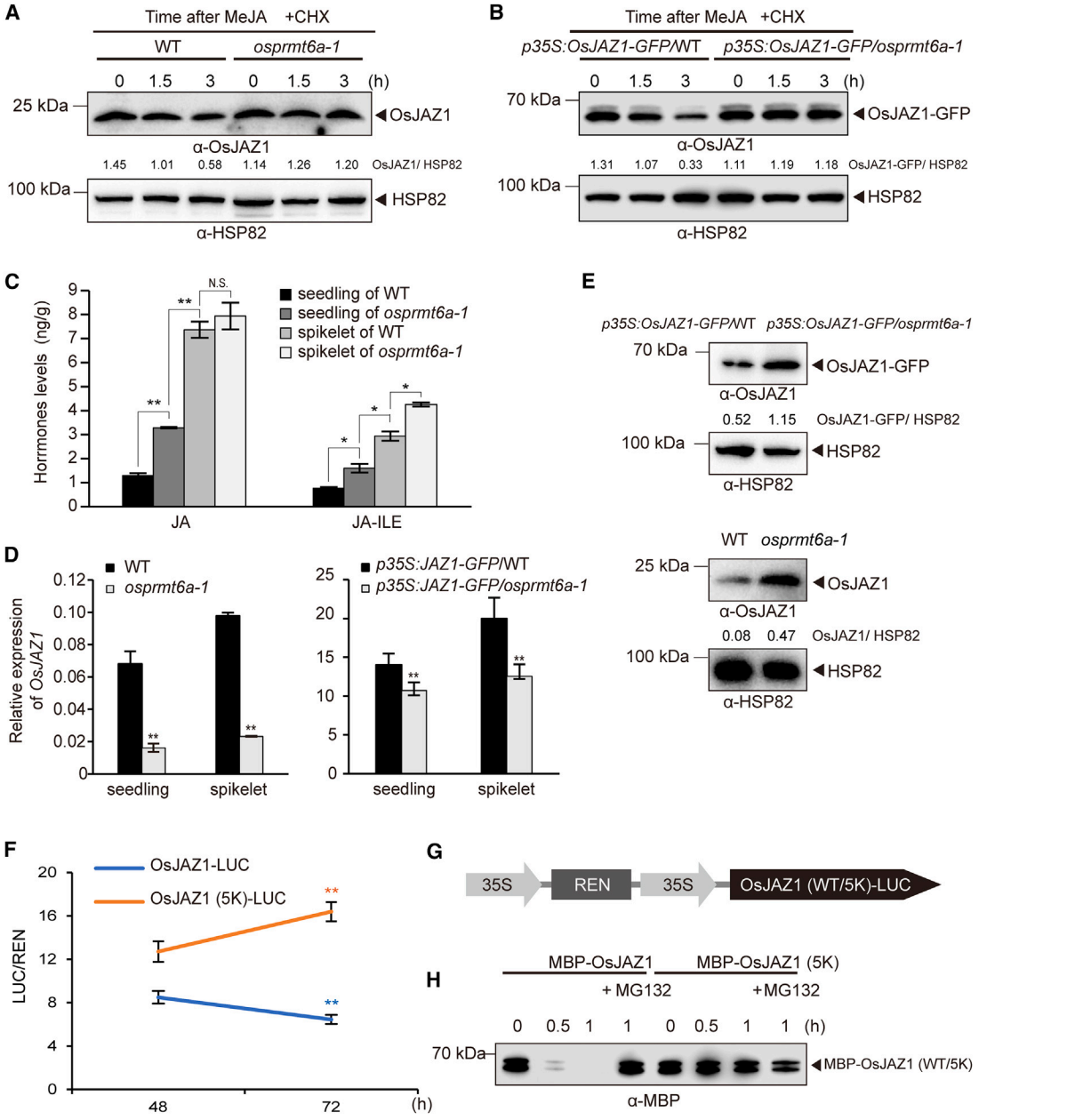

Figure 3. JAs promote OsJAZ1 degradation in the presence of OsPRMT6a.

(A and B) Western blot analysis reveals that 2 mM MeJA induces OsJAZ1 degradation in WT but not in *osprmt6a-1* transgenic plants or OsJAZ1-GFP degradation in *p35S:OsJAZ1-GFP*/WT but not in *p35S:OsJAZ1-GFP/osprmt6a-1* transgenic plants.

(C) Levels of JA and its amino acid derivative JA-Ile in seedlings and spikelets of WT and *osprmt6a-1*.

(D) Expression levels of *OsJAZ1* in 2-week-old seedlings or spikelets of the WT and *osprmt6a-1*, *p35S:OsJAZ1-GFP*/WT, and *p35S:OsJAZ1-GFP/osprmt6a-1* transgenic plants.

(E) Protein levels of OsJAZ1 in spikelets of WT and *osprmt6a-1* plants or of OsJAZ1-GFP in spikelets of *p35S:OsJAZ1-GFP*/WT and *p35S:OsJAZ1-GFP/osprmt6a-1* transgenic plants.

(F) *In vivo* dual-LUC-degradation assay using luciferase reporters, OsJAZ1-LUC and OsJAZ1 (5K)-LUC, transiently expressed in *N. benthamiana* leaves for 48 h and 72 h, respectively. Values are means ± SEM ($n = 3$ replicates). Asterisks denote statistically significant differences between samples (*$p < 0.05$, **$p < 0.01$ by Student's *t*-test).

(G) Schematic representation of the OsJAZ1-LUC and OsJAZ1 (5K)-LUC constructs for the dual-LUC-degradation assay in **(C)**. 35S, CaMV35S promoter; REN, *Renilla* luciferase; OsJAZ1(WT/5K)-LUC, fusion protein of OsJAZ1 (or OsJAZ1 (5K)) and Firefly luciferase.

(H) Cell-free degradation assay showing that MBP-OsJAZ1 is more easily degraded than MBP-OsJAZ1 (5K) and that the proteasome inhibitor MG132 inhibits degradation of MBP-OsJAZ1.

Numbers below the western blot images represent the band density ratio of α-OsJAZ1/α-HSP82 **(A, B, and E)** as quantified using ImageJ.

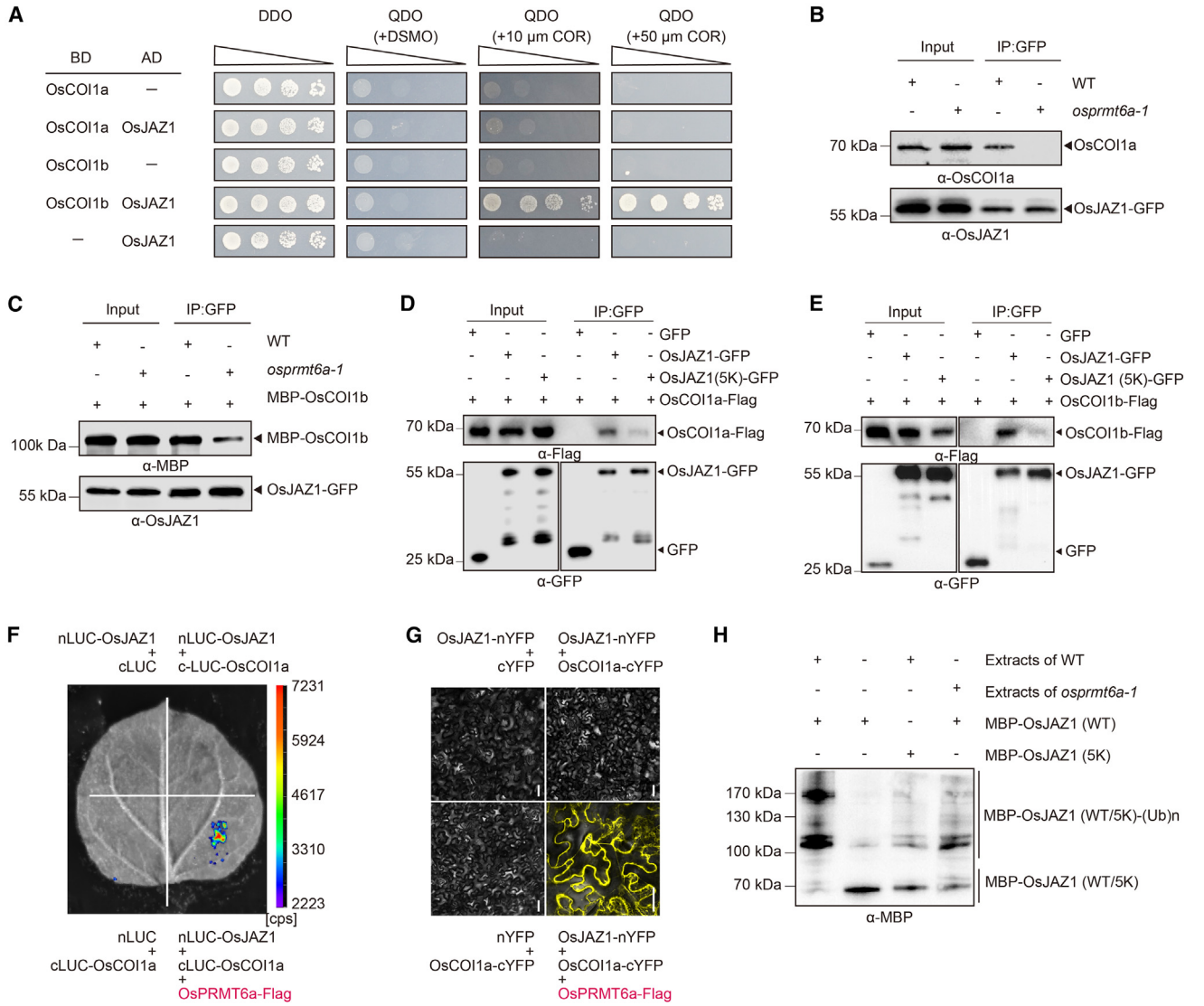

Figure 4. OsPRMT6A promotes the interaction of OsJAZ1 with OsCOI1a or OsCOI1b to facilitate OsJAZ1 ubiquitination.

(A) Y2H assay showing the interaction of OsCOI1b with OsJAZ1 in the presence of coronatine (COR) at different concentrations, no interaction of OsCOI1b with OsJAZ1 in the absence of COR, and no interaction of OsJAZ1 with OsCOI1a in the presence or absence of COR. BD, binding domain; AD, activating domain; the gradients indicate 10-fold serial dilutions.

(B) *In vivo* Co-IP showing the interaction between OsCOI1a and OsJAZ1-GFP in the WT and *osprmt6a-1* backgrounds. OsJAZ1-GFP in WT or *osprmt6a-1* was used as bait to immunoprecipitate native OsCOI1a.

(C) Semi-*in vivo* Co-IP showing the interaction between MBP-OsCOI1b and OsJAZ1-GFP in the WT and *osprmt6a-1* backgrounds. OsJAZ1-GFP in WT or *osprmt6a-1* was used as bait to immunoprecipitate the exogenously added prokaryotically expressed MBP-OsCOI1b.

(D and E) *In vivo* Co-IP showing the stronger interaction of OsCOI1a-FLAG or OsCOI1b-FLAG with OsJAZ1-GFP than with OsJAZ1 (5K)-GFP in rice protoplasts. OsJAZ1-GFP or OsJAZ1-GFP (5K) was used as bait to immunoprecipitate OsCOI1a-FLAG or OsCOI1b-FLAG.

(F) LCI assay shows that the interaction between OsPRMT6a and OsJAZ1 depends on OsPRMT6a in *N. benthamiana* leaves. The pseudocolor bar (right panel) shows the range of luminescence intensity in each image.

(G) BiFC assay showing that the interaction between OsPRMT6a and OsJAZ1 depends on OsPRMT6a in leaf epidermal cells of *N. benthamiana*.

(H) *In vitro* ubiquitination assay showing greater ubiquitination of OsJAZ1 by WT than by *osprmt6a-1* plant extracts but that OsJAZ1 (5K) exhibits weak ubiquitination by WT plant extracts.

The symbols "–" and "+" denote the absence and presence of the corresponding proteins. Scale bars, 50 μm.

BiFC assay revealed an interaction between OsCOI1a and OsJAZ1 in the absence of OsPRMT6a, as reported previously (Cai et al., 2014; Cao et al., 2021); however, when OsPRMT6a was coexpressed, both assays revealed an interaction (Figure 4F and 4G), indicating that the interaction between OsJAZ1 and OsCOI1a *in vivo* depends on OsPRMT6a.

OsJAZ1 suppresses JA signaling by interacting with OsMYC2 in the absence of JAs. Therefore, to assess whether the arginine methylation of OsJAZ1 affects the interaction of OsJAZ1 with OsMYC2, we performed a Y2H assay. The results indicated that both OsJAZ1 and OsJAZ1 (5K) exhibited similar abilities to bind to OsMYC2 (Supplemental Figure 16), suggesting that

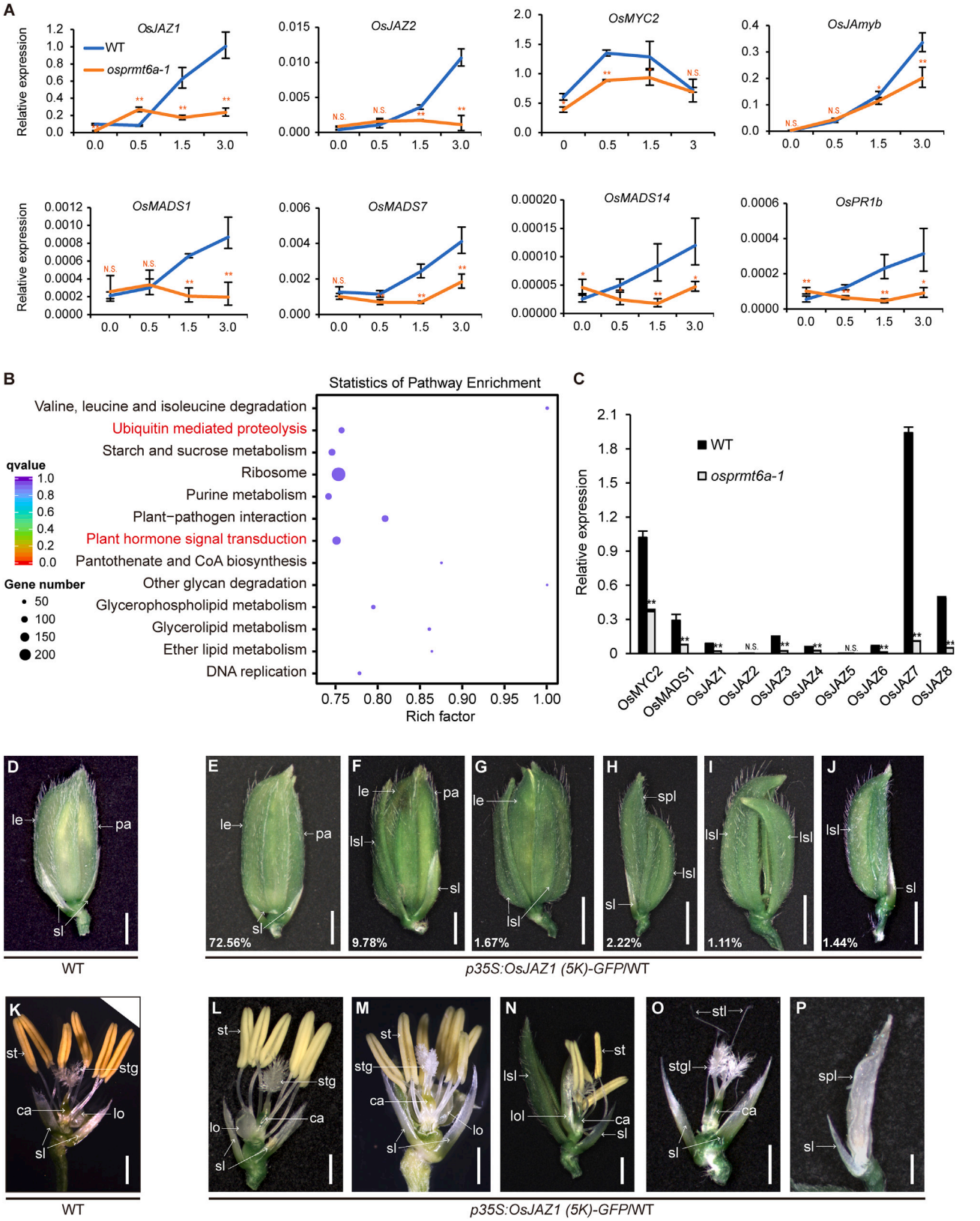

Figure 5. The arginine demethylation status of OsJAZ1 impedes JA responses and normal spikelet development.

(A) Expression changes in JA signaling pathway genes. The horizontal axis of the line chart is the sampling time of 25-day-old seedlings after 2 mM MeJA treatment.

(legend continued on next page)

arginine methylation of OsJAZ1 does not affect the interaction of OsJAZ1 with OsMYC2.

We next performed an *in vitro ubiquitination assay* using MBP-OsJAZ1 and MBP-OsJAZ1 (5K) proteins expressed in *Escherichia coli*. The results revealed a decrease in ubiquitinated MBP-OsJAZ1 proteins in *osprmt6a-1* plant extracts or MBP-OsJAZ1 (5K) proteins in WT plant extracts compared with ubiquitinated MBP-OsJAZ1 in WT plant extracts (Figure 4H). These results indicate that the arginine methylation of OsJAZ1 by OsPRMT6a promotes the interaction of OsJAZ1 with OsCOI1a and OsCOI1b, subsequently facilitating OsJAZ1 ubiquitination.

Consistent with these findings, *oscoi1a oscoi1b* double-mutant plants also exhibited abnormal spikelet morphology similar to that observed in *osprmt6a* plants (Supplemental Figure 17), supporting the conclusion that arginine methylation of OsJAZ1 enhances its interaction with OsCOI1a or OsCOI1b, promoting OsJAZ1 ubiquitination and ultimately influencing spikelet development.

Stabilization of OsJAZ1 due to loss of arginine methylation impedes JA responses and normal spikelet development

In *Arabidopsis*, both JAZ-overexpressing and JAZ-knockout plants exhibit abnormal responses to JAs (Yan et al., 2014; Guo et al., 2018). To investigate whether the stabilization of OsJAZ1 in *osprmt6a-1* leads to abnormal JA responses, we treated the WT and *osprmt6a-1* plants with 2 mM MeJA and observed their responses by analyzing changes in the expression of JA-responsive genes. The results indicated reduced expression of these JA signaling genes in *osprmt6a-1* relative to WT seedlings (Figure 5A), signifying diminished JA responses in *osprmt6a-1* compared with the WT. To analyze differences in gene expression between the WT and *osprmt6a-1* under normal conditions, we performed a global RNA sequencing (RNA-seq) analysis using RNA extracted from approximately 1-cm-long inflorescences. Cluster analysis revealed differences in the expression of thousands of genes, including 17 genes related to the JA signaling pathway, 90 genes related to ubiquitin-mediated proteolysis, and numerous other genes involved in plant development (Supplemental Data 1). RT–qPCR analyses confirmed significant reductions in the expression of many genes related to the JA signaling pathway in *osprmt6a-1* compared with the WT, validating the RNA-seq results (Figure 5B and 5C). Together, these findings support the notion that stabilized OsJAZ1 (and possibly other OsJAZs) in *osprmt6a-1* diminishes JA responses.

Previous studies have demonstrated that nondegradable JAZ variants lead to abnormal spikelet development by reducing JA responses (Cai et al., 2014; Hori et al., 2014; Cao et al., 2021). To investigate whether stabilization of OsJAZ1 by the loss of arginine methylation has similar effects on spikelet development, we generated *p35S*:*OsJAZ1* (*1K*)-*GFP*/WT and *p35S*:*OsJAZ1* (*5K*)-*GFP*/WT transgenic plants from the japonica rice cultivar Kitaake for genetic analysis. As anticipated, the *p35S*:*OsJAZ1* (*5K*)-*GFP*/WT transgenic plants exhibited abnormal spikelets resembling those of *osprmt6a* plants (Figure 5D–5P), whereas the *p35S*:*OsJAZ1*-*GFP*/WT and *p35S*:*OsJAZ1* (*1K*)-*GFP*/WT transgenic plants did not exhibit any abnormal phenotypes (Supplemental Figure 18), indicating that the 1K modification of OsJAZ1 is insufficient to mediate the regulatory effect of OsPRMT6a on spikelet development. Overall, the similar spikelet abnormalities of the *osprmt6a* and *p35S*:*OsJAZ1* (*5K*)-*GFP*/WT transgenic plants suggests that abnormal spikelet development in *osprmt6a* likely results from the absence of arginine methylation in OsJAZ1.

JA signaling represses the expression of *OsPRMT6a* through OsMYC2

Because negative feedback commonly occurs in hormone regulation, we sought to investigate whether JA signaling influences the expression of *OsPRMT6a*. To explore this possibility, WT seedlings were treated with 1 mM MeJA and sampled at specific time points, after which mRNA and protein levels were measured by RT–qPCR and western blotting, respectively. The results revealed a reduction in both the mRNA and protein levels of *OsPRMT6a* following MeJA treatment (Figure 6A and 6B).

We next aimed to identify the transcription factor that directly represses *OsPRMT6a* expression in response to JAs. By analyzing the promoter sequence of *OsPRMT6a* with PlantCARE, an online database of *cis*-acting regulatory elements in plants (Lescot et al., 2002), we identified six recognizable motifs (P1–P6) of the MYC family in the promoter and intron of *OsPRMT6a* (Figure 6C). Given that MYC2 is a crucial regulator of JA-responsive genes (Chini et al., 2007), we used a chromatin immunoprecipitation (ChIP)–qPCR assay to investigate whether OsMYC2 (the rice homolog of MYC2) could bind to the promoter of *OsPRMT6a*. To express the OsMYC2-GFP fusion protein, along with the *OsPRMT6a* promoter and coding sequence, we generated two transient expression

(B) RNA-seq analysis of WT vs. *osprmt6a-1* and KEGG pathways enriched in the differentially expressed genes.
(C) RT–qPCR results confirm the clustering results of the RNA-seq analysis regarding the JA signaling pathway. Values are presented as means ± SEM (n = 3 replicates). Asterisks represent statistically significant differences in the relative expression of the corresponding genes between WT and *osprmt6a-1* at the same time point, and "N.S." denotes no significant difference (*$p < 0.05$, **$p < 0.01$ by Student's t-test).
(D–J) Spikelet morphologies, including normal spikelets in the WT **(D)** and various spikelet morphologies in *p35S: OsJAZ1 (5K)-GFP/WT transgenic plants, including* normal spikelet **(E)**, abnormal spikelets with long sterile lemma **(F)**, two long sterile lemmas **(G)**, a long sterile lemma and a spikelet-like structure **(H)**, two separate long sterile lemmas **(I)**, and one separate long sterile lemma **(J)**. The ratio of the specific mutation type is marked in the lower left corner.
(K) WT floret with six stamens, two lodicules, one carpel, and two stigmas. The lemma and palea were removed.
(L–P) *p35S*: *OsJAZ1* (*5K*)-*GFP*/WT transgenic plants with normal florets like those of the WT **(L)** and abnormal florets with seven stamens **(M)**, a long sterile lemma and lodicule-like structure **(N)**, three stamens and a stigma-like structure **(O)**, or a spikelet-like structure **(P)**.
le, lemma; pa, palea; st, stamen; stl, stamen-like structure; sl, sterile lemma; lo, lodicule; stg, stigma; stgl, stigma-like structure; lsl, long sterile lemma; spl, spikelet-like structure; ca, carpel; cal, carpel-like structure; lol, lodicule-like structure. Scale bars, 2 mm **(D–J) and 1 mm (K–P).**

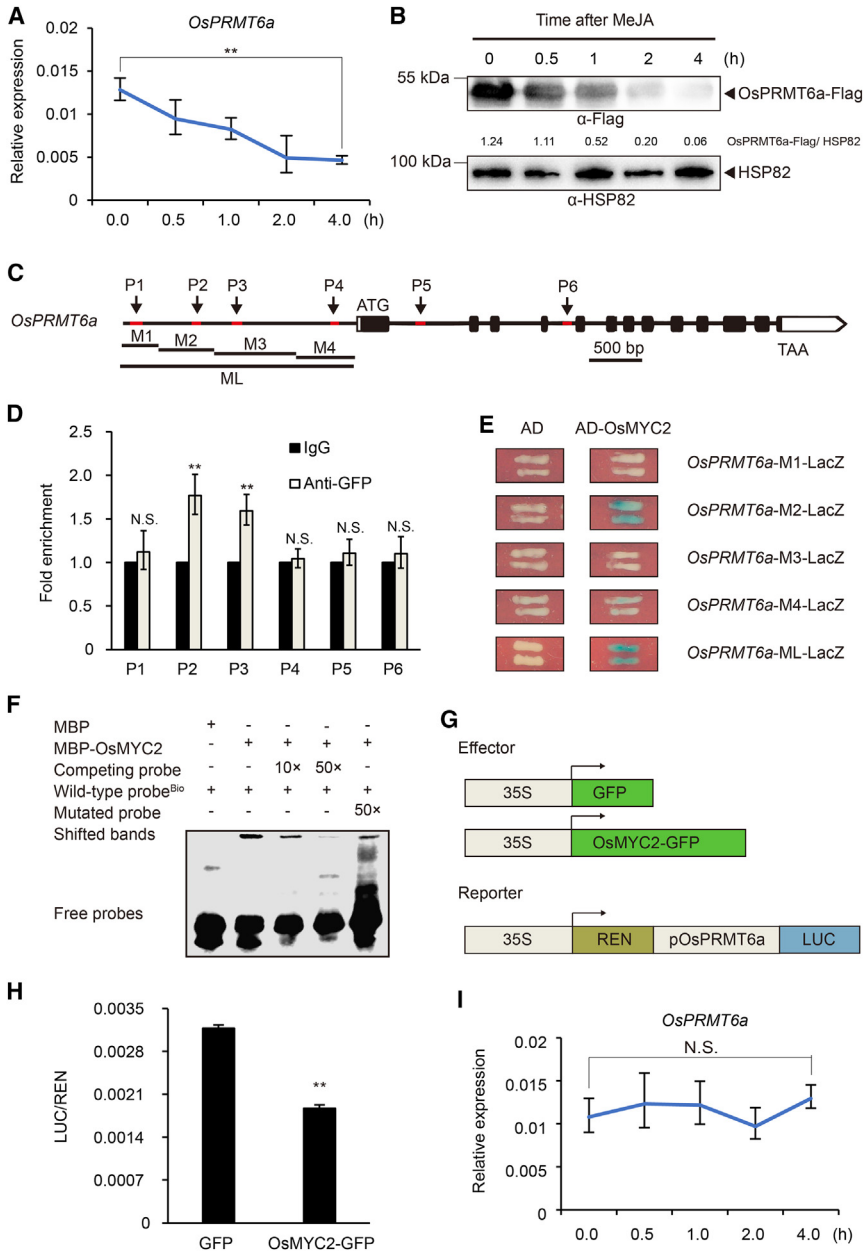

Figure 6. MeJA represses *OsPRMT6a* expression through OsMYC2.

(A) The mRNA level of *OsPRMT6a* decreases following 1 mM MeJA treatment in 12-day-old WT seedlings.

(B) Protein level of OsPRMT6a decreases following 1 mM MeJA treatment in 12-day-old *pUbi*:*OsPRMT6a-FLAG* transgenic plants. Numbers below the images represent the band density ratio of α-FLAG/α-HSP82 quantified with ImageJ software.

(C) Diagram of the *OsPRMT6a* genomic region featuring DNA fragments (red lines, P1–P6) with the G-box (5′-CACGTG/CACATG-3′) motif. White boxes, untranslated regions; black boxes, exons; black lines, introns.

(D) ChIP–qPCR analysis showing amplification of promoter fragments P2 and P3 from immunoprecipitation pulled down by the anti-GFP antibody. The control, immunoglobulin G, was set to 1.

(E) Y1H assays of the binding regions of OsMYC2 in the promoter regions of *OsPRMT6a*. A series of promoter fragments of *OsPRMT6a* were fused to the upstream region of the LacZ reporter gene for the OsMYC2 binding test. AD, the empty pB42AD negative control.

(F) EMSA assay showing direct binding of OsMYC2 to the G-box motif in the *OsPRMT6a* promoter. The arrow indicates the shifted band representing the protein–DNA complex. The symbols "−" and "+" denote the absence and presence of the corresponding proteins or probes.

(G) Schematic representation of the effector and reporter constructs. Full-length CDSs of the OsMYC2-GFP fusion protein or GFP protein under the control of the 35S promoter acted as effectors. The firefly luciferase gene *LUC* driven by the *OsPRMT6a* promoter and the *Renilla* luciferase gene *REN* driven by the 35S promoter acted as the reporters.

(H) Transient dual-LUC reporter assays revealing OsMYC2 inhibition of *OsPRMT6a* transcription.

(I) The mRNA level of *OsPRMT6a* remained relatively unchanged in the loss-of-function mutant *osmyc2* upon treatment of 12-day-old seedlings with 1 mM MeJA.

Values are means ± SEM ($n = 3$ replicates). Asterisks indicate significant differences, and "N.S." denotes no significant difference (**$p < 0.01$ by Student's *t*-test) **(A, D, H, I)**.

vectors and infected tobacco leaves via *Agrobacterium*-mediated transformation. The ChIP–qPCR results indicated that P2 and P3, but not P1, P4, P5, or P6, were amplified from immunoprecipitates pulled down by the anti-GFP antibody (Figure 6D). Yeast one-hybrid (Y1H) assays revealed that OsMYC2 could bind to the P2 region in the *OsPRMT6a* promoter (Figure 6E). In addition, we performed a DNA electrophoretic mobility shift assay (EMSA) to determine whether OsMYC2 directly regulates *OsPRMT6a* transcription by binding to the G-box motif (5′-CACGTG-3′) of P2 *in vitro*. The results showed that the MBP-OsMYC2 fusion protein, rather than the free MBP protein, bound specifically to the DNA probe that contained P2 with one G-box motif (Figure 6F). Furthermore, a LUC reporter assay demonstrated that *OsPRMT6a* promoter-driven LUC expression was repressed by OsMYC2-GFP (Figure 6G and 6H). To genetically confirm that the regulation of *OsPRMT6a* by JAs is dependent on OsMYC2, we generated the loss-of-function mutant *osmyc2* by CRISPR/Cas9 technology and found that this mutant, similar to the *osprmt6a* mutants, also displayed abnormal spikelet structures (Supplemental Figure 19). Under 1 mM MeJA treatment, the *OsPRMT6a* mRNA level did not decrease in *osmyc2* (Figure 6I), in contrast to the reduction observed in the WT (Figure 6A). These results suggest that JAs likely repress the expression of *OsPRMT6a* through OsMYC2.

Negative correlation between OsJAZ1 arginine methylation level and high temperature

After a 3-year investigation of the rate of spikelet abnormality in Shunyi district, Beijing, we found that the rate of spikelet

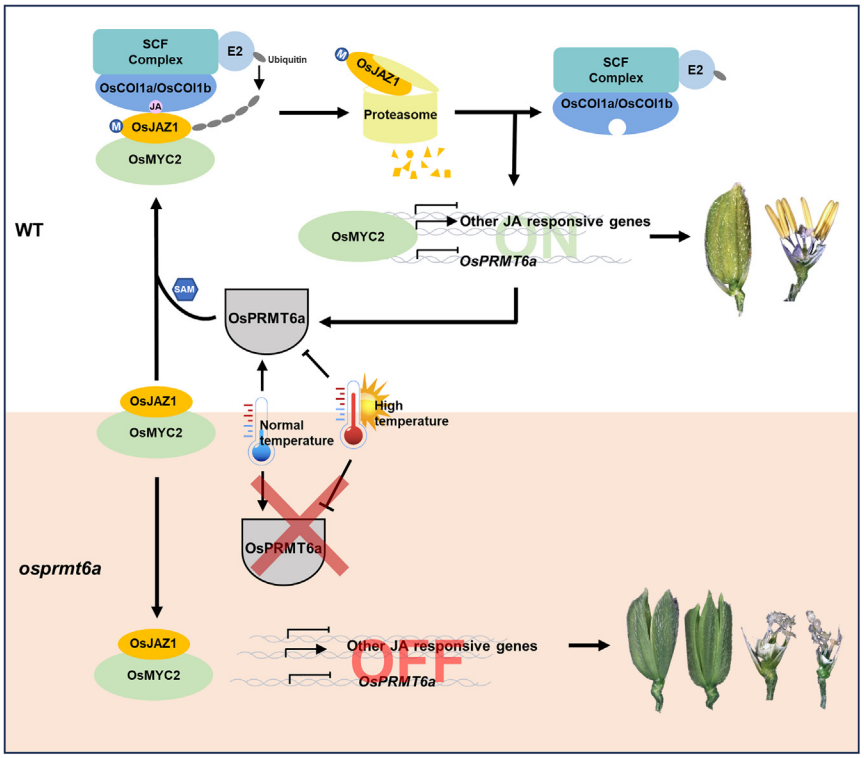

Figure 7. Schematic model illustrating how arginine methylation of OsJAZ1 by OsPRMT6a promotes OsJAZ1 degradation and thus JA signal transmission.
In the WT, OsPRMT6a methylates arginines of OsJAZ1. The arginine methylation of OsJAZ1 enhances its interaction with OsCOI1a/OsCOI1b, thus promoting the ubiquitination of OsJAZ1 by the $SCF^{OsCOI1a/OsCOI1b}$ complex and subsequently the degradation of OsJAZ1 by the 26S proteasome. The degradation of OsJAZ1 frees OsMYC2 to activate (or repress) JA-responsive genes, including *OsPRMT6a*, ultimately promoting the transmission of the JA signal to maintain normal spikelet development. The OsPRMT6a protein accumulates at normal temperatures but decreases at high temperatures, leading to dynamic changes in OsPRMT6a-regulated arginine methylation and OsJAZ1 protein level with temperature fluctuations. SAM, methyl donor *S*-adenosylmethionine; M, methyl. However, in loss-of-function *osprmt6a* mutants, dynamic changes in OsPRMT6a-regulated arginine methylation and OsJAZ1 protein level do not occur, leading to constant stabilization of OsJAZ1. This stabilization hinders JA signal transduction, ultimately causing abnormal spikelet development.

abnormality was lower in *osprmt6a-1* in 2021 than in 2020 and 2022 (Supplemental Table 1). The critical period for spikelet formation in the Shunyi district occurs in July. To explore whether climatic differences were responsible for differences in rates of spikelet abnormality of *osprmt6a-1* between 2021 and 2020 or 2022, we obtained climate data for July from a Chinese weather website (https://www.tianqi.com/). In July 2020, the average maximum and minimum temperatures were 31°C and 22°C, respectively, with a minimum temperature of 20°C and seven overcast or rainy days. In July 2022, the average maximum and minimum temperatures were 32°C and 22°C, respectively, with a minimum temperature of 20°C and six overcast or rainy days. By contrast, in July 2021, the average maximum and minimum temperatures were 29°C and 22°C, respectively, with a minimum temperature of 18°C and 18 overcast or rainy days (Supplemental Table 2). These data suggested that *osprmt6a-1* spikelet abnormalities occurred more readily on sunny days with higher temperatures than on rainy days with lower temperatures (Supplemental Tables 1 and 2). In line with this observation, we observed negative correlations of high temperature with both OsPRMT6a protein level and OsJAZ1-GFP arginine methylation level but a positive correlation of high temperature with of OsJAZ1-GFP protein level in the *p35S*:*OsJAZ1-GFP*/WT transgenic plants; however, these dynamic changes were absent in the *p35S*:*OsJAZ1-GFP*/*osprmt6a-1* transgenic plants (Supplemental Figure 20A).

To alleviate the influence of environmental factors and circadian rhythms that likely affect JA biosynthesis and signaling (Thines et al., 2019), we planted *p35S*:*OsJAZ1-GFP*/WT and *p35S*:*OsJAZ1-GFP*/*osprmt6a-1* in different growth chambers (with different temperatures) and collected the spikelets at 10 a.m. Similar results confirmed that there was indeed a negative correlation between OsJAZ1 arginine methylation level and high temperature (Supplemental Figure 20B). We also planted WT and *osprmt6a-1* plants in different growth chambers to mimic natural temperature changes (Supplemental Table 4) and observed the formation of abnormal spikelets. The results showed that mimicking a relatively high natural temperature caused a greater percentage of abnormal spikelets than did mimicking a relatively low natural normal temperature (Supplemental Table 5), providing genetic evidence that OsPRMT6a-mediated arginine methylation likely facilitates normal spikelet development under high-temperature conditions.

DISCUSSION

Our study revealed a pivotal role for OsPRMT6a in the maintenance of normal spikelet development. We propose a model in which OsPRMT6a methylates arginine residues of OsJAZ1, enhancing their interaction with the JA receptors OsCOI1a and OsCOI1b. This interaction triggers the ubiquitination and subsequent degradation of OsJAZ1, ensuring efficient JA signal transduction (Figure 7). By establishing a molecular link between JA signaling and arginine methylation, our findings not only shed new light on the transduction mechanism and self-balancing nature of JA signaling but also provide insights into the intricate interplay between arginine methylation and key regulators of plant defense and development.

Previous reports have highlighted the effect of protein arginine methylation on protein stability via modulation of substrate phosphorylation levels and direct effects on protein–protein interactions (Yamagata et al., 2008; Bedford and Clarke, 2009; Estève

et al., 2011; Fang et al., 2014). Our study provides a novel perspective, demonstrating that arginine methylation influences protein stability. OsPRMT6a-catalyzed arginine methylation of OsJAZ1 primarily affects stability by modulating the interaction of OsJAZ1 with OsCOI1a and OsCOI1b, ultimately leading to ubiquitination by the $SCF^{OsCOI1a/OsCOI1b}$ complex (Figure 4). Eukaryotic proteins undergo various post-translational modifications at different stages of their functions, and these modifications interact with each other to produce diverse biological effects. Previous studies have emphasized the interplay between protein arginine methylation and other modifications, such as phosphorylation (Yang et al., 2010; Carr et al., 2011) and acetylation (Ivanov et al., 2007). Our research established a direct link between protein arginine methylation and ubiquitination, providing novel insights into the intricate mechanisms of JA signaling.

Notably, in the absence of JAs, OsJAZ1 can still undergo arginine methylation, which does not impede its binding to OsMYC2, thus maintaining its repression of JA signaling. When abundant JA is present, arginine methylation of OsJAZ1 efficiently promotes its interaction with the $SCF^{OsCOI1a/OsCOI1b}$ complex, leading to OsJAZ1 ubiquitination and degradation and ultimately to efficient transmission of the JA signal (Figures 2, 3, 4, and 5; Supplemental Figures 14–18). Constitutive high levels of many plant hormones are harmful to plant growth and development; thus, plants use a variety of negative feedback mechanisms to finely tune their hormonal signaling strength (Tong et al., 2009; Wolters and Jurgens, 2009; Wu et al., 2016; Chico et al., 2020). Here, we also discovered that a negative feedback pathway, OsPRMT6a–OsJAZ1–OsMYC2–*OsPRMT6a*, likely attenuates the OsPRMT6a-mediated arginine methylation of OsJAZ1 by repressing OsPRMT6a expression to tune down JA signaling (Figure 6). These findings suggest that OsPRMT6a-mediated arginine methylation likely acts as a switch to fine-tune JA signaling.

The significance of protein arginine methylation is underscored by the comprehensive abnormal phenotypes observed in loss-of-function *osprmt6a* mutants. These mutants exhibit dwarfism, increased tiller number, reduced seed setting, abnormal floret organs, disrupted seed dormancy, and altered responses to various hormones, among other characteristics (Supplemental Figure 2). These findings imply that PRMTs, particularly OsPRMT6a, may have numerous substrates that play vital roles in regulating plant growth and development. Furthermore, protein arginine methylation, by diversifying protein forms without altering the amino acid sequence, contributes to the "protein epigenetic universe," enabling intricate regulatory functions in organisms. Thus, our study provides new insights for exploring additional PRMT substrates, including those of OsPRMT6a, to unravel the complex regulatory networks that govern life processes. In addition, the well-established link between organism adaptability and protein arginine methylation (Zhang et al., 2011) and the findings of our study (Supplemental Figure 20 and Supplemental Tables 1–5) suggest that OsPRMT6a-mediated arginine methylation likely acts as a switch to epigenetically fine-tune JA signaling, ensuring the adaptation of rice development (including spikelet development) to harsh environmental conditions such as high temperature.

METHODS

Plant materials and growth conditions

The WT (the japonica rice cultivar Kitaake) and *osprmt6a* mutants were cultivated during the natural growing season in an experimental field located in the Shunyi district of Beijing. For RT–qPCR, protein quantitative assays, and MeJA treatment assays, the WT and mutant seedlings were cultivated in climate chambers (HP1500GS, Ruihua) under long-day conditions comprising daily cycles of 14 h light at 30°C and 10 h darkness at 25°C, along with 70% humidity. The light source consisted of fluorescent white light tubes (400–700 nm, 250 μmol m^{-2} s^{-1}).

The developmental stages of the rice spikelets were determined according to previously described methods (Ikeda et al., 2004).

Overlap extension PCR-based cloning

To obtain the OsJAZ1 protein variants (1K/5K), we used overlap extension PCR to introduce base mutation sites. To generate the *p35S*:*OsJAZ1* (5K)-*GFP* constructs, the primers GFP-JAZ1F and GFP-JAZ1R, along with the base mutation primer pair, were used to amplify the PCR fragment in segments. Subsequently, the complete PCR product of OsJAZ1 (5K) was amplified with the primers GFP-JAZ1F and GFP-JAZ1R, using the previously segmented PCR fragment containing the base mutation sites as a template. The PCR products were cloned and inserted into the binary vector pCAMBIA1305-GFP using the In-Fusion Advantage PCR Cloning Kit (Clontech). The *p35S*:*OsJAZ1* (*1K*)-*GFP*, *pGADT7-OsJAZ1* (*5K*), and *pMalc2x-OsJAZ1* (*5K*) constructs were obtained using the same methods.

Vector construction and plant transformation

To generate knockout lines for *OsPRMT6a* and *OsMYC2*, an 18-bp gene-specific fragment with NGG at its 3′ end was inserted into the CRISPR/Cas9 expression vector (Lei et al., 2014).

Com-OsPRMT6a lines were produced by cloning a 7-kb full-length *OsPRMT6a* gene fragment into the pCAMBIA1305.1 vector to complement the *osprmt6a* phenotype.

For *OsPRMT6a* gene knockdown, two inverted repeats of a 304-bp sequence were amplified with a primer pair and then cloned and inserted into the pCUbi1390-ΔFAD2 vector in the sense and antisense orientations using the *Xho*I/*Kpn*I and *Bam*HI/*Xba*I sites to create the RNAi construct *pUbi*:*dsRNAi-OsPRMT6a*.

To generate *OsPRMT6a*-overexpressing transgenic plants, the 1188-bp coding sequence (CDS) of *OsPRMT6a* was inserted into the *Acc65I* restriction site in the pCAMBIA1390-FLAG overexpression vector driven by a maize ubiquitin promoter to obtain the *pCAMBIA1390-PRMT6a-FLAG* construct.

To construct *p35S*:*OSJAZ1-GFP*, the 654-bp CDS of *OsJAZ1* was amplified with primers, and the PCR products were then inserted into the binary vector pCAMBIA1305-GFP using an In-Fusion Advantage PCR Cloning Kit (Clontech). The *p35S*:*OsJAZ1* (*5K*)-*GFP* constructs were also created using the same method. Finally, the *p35S*:*OSJAZ1-GFP* and *p35S*:*OsJAZ1* (*5K*)-*GFP* constructs were introduced into the WT variety Kitaake, and the

p35S:OSJAZ1-GFP construct was also introduced into *osprmt6a-1*.

All transgenic rice plants were generated via *Agrobacterium*-mediated transformation of rice calli, as described previously (Hiei et al., 1994). The material for the *oscoi1a oscoi1b* double mutant was provided by Dr. Dong-Lei Yang's research group at Nanjing Agricultural University.

Cytological observation

To prepare semi-thin sections, panicles of *osprmt6a and WT plants* at various developmental stages were fixed in Carnoy's solution (75% alcohol, 25% acetic acid), then dehydrated through a gradient of 30%, 50%, 70%, 85%, 90%, 95%, and 100% acetone for 15 min each. Following dehydration, the samples were infiltrated with 25%, 50%, and 75% resin for 3 h, followed by the addition of pure resin for 12 h. After incubation at 35°C and 45°C for 12 h each and then at 60°C for 48 h, the embedded material surrounding the sample was trimmed into a trapezoid shape to facilitate sample exposure. The samples were sectioned into 1-μm slices using an ultramicrotome and mounted on glass slides. The sections were stained with 0.5% toluidine blue, washed with water, and observed under a Nikon Eclipse E80i light microscope.

For scanning electron microscopy, spikelets at early developmental stages were fixed overnight at 4°C using a 2.5% glutaraldehyde solution and processed as described previously (Mou et al., 2000).

RNA extraction and RT–qPCR

Total RNA was extracted from various tissues using the ZR Plant RNA MiniPrep Kit (Zymo Research). Subsequently, 1 μg of total RNA was subjected to a 20-μl reverse transcription reaction with a PrimeScript reverse transcriptase kit (TaKaRa, Shiga, Japan). RT–qPCR analyses were performed in an ABI 7500 real-time PCR system with the SYBR Premix Ex Taq Kit (TaKaRa). The rice ubiquitin gene (UBQ, Os03g0234200) served as a reference gene for normalization. The $2^{-\Delta\Delta Ct}$ method was used to analyze relative gene expression levels. The sequences of primers used in this and subsequent assays are listed in Supplemental Table 4.

Statistical analysis

Student's *t*-test was used to compare the means of two independent groups. Fisher's least significant difference test was used to compare multiple means.

RNA *in situ* hybridization

A 247-bp gene-specific cDNA fragment containing the *OsPRMT6a* CDS was amplified, cloned, and inserted into the pGEM-T Easy vector (Promega). RNA *in situ* hybridization was performed following a previously described procedure (Li et al., 2011).

Subcellular localization

To ascertain the subcellular localization of the OsPRMT6a protein, the coding region of *OsPRMT6a* spanning 1188 bp was fused upstream of GFP in the transient expression vector pAN580 using the *Xba*I and *Bam*HI restriction sites. The resulting PAN580-6A construct was driven by the double CaMV35S promoter. Using an established protocol (Cai et al., 2014), rice protoplasts were transfected with the PAN580-6A plasmid to examine the localization of the OsPRMT6a protein within the cell. GFP fluorescence was observed using a confocal laser scanning microscope (LSM 980; Zeiss).

Phylogenetic analysis and homologous sequence alignment

We performed a phylogenetic analysis using the protein sequences of all known PRMTs from *Arabidopsis* and rice. In addition, protein sequences of OsPRMT6a orthologs from 23 other species, selected using an E-value threshold of less than $1e^{-180}$, were retrieved from the National Center for Biotechnology Information (NCBI) database (https://www.ncbi.nlm.nih.gov/). A phylogenetic tree with 1000 bootstrap replicates was constructed using the neighbor-joining method implemented in MEGA 11.0.10 software and refined using the EvolView website (https://www.evolgenius.info/evolview/#/).

The protein sequences used for sequence alignment included OsPRMT6a and OSPRMT6b from *O. sativa*, AtPRMT6 from *A. thaliana*, BRADI3g29470 from *Brachypodium distachyon*, SORBI3001G211900 from *Sorghum bicolor*, and GRMZM2G 160752 from *Zea mays*. Sequence alignment was performed using BioEdit software.

Yeast two-hybrid assay

The GAL4 binding domain was used to fuse the coding sequences of *OsPRMT6a*, *OsMYC2*, and *OsCOI1b* into the *Eco*RI and *Bam*HI restriction sites of the pGBKT7 vector, which was designated the "bait" vector. A cDNA library from young rice inflorescences was screened using a Y2H assay, and positive clones were identified by sequencing. The CDSs of 15 members of the rice JAZ family were inserted into the *Eco*RI and *Bam*HI restriction sites of the pGADT7 vector from Clontech, designated the "prey" vector. Negative controls were established using the empty pGBKT7 and pGADT7 vectors. The Yeast Protocols Handbook (Clontech) was consulted for detailed experimental procedures.

Protein electrophoresis and western blotting

Denatured proteins were separated on SDS–PAGE gels and detected by western blotting analysis with the appropriate antibodies. The detailed methods have been described previously (Lin et al., 2012; Zhou et al., 2013).

For western blotting analysis, we used HSP82 as the internal standard to ensure consistent protein loading across different samples. Western blot bands were quantified with the image analysis software ImageJ (Taylor et al., 2013). Images were obtained with a ChemiDoc MP Imaging System (Bio-Rad) or an Odyssey 2800 imaging system (LI-COR).

Antibody preparation

To detect OsJAZ1, the full-length CDS of *OsJAZ1* was amplified, cloned, and inserted into the PGEX-4T-AB1 vector (Supplemental Table 5). The resulting protein, GST-OsJAZ1, was expressed in *E. coli* BL21 (DE3, TransGen) cells and subjected to affinity purification. The recombinant protein was then

used to generate polyclonal antibodies against OsJAZ1 in rabbits (ABclonal).

In vivo coimmunoprecipitation assay

The p35S:OSJAZ1-GFP vector was used for the *in vivo* Co-IP assay. The full-length coding regions of *OsJAZ7* and *OsJAZ8* were separately cloned and inserted into the pCAMBIA1305-GFP vector to produce *p35S*:*OsJAZ1-GFP* (*5K*), *p35S*:*OsJAZ7-GFP*, and *p35S*:*JAZ8-GFP*, respectively. The full-length CDS of *OsPRMT6a* was inserted into the pCUbi1390 vector to produce *pUbi*:*OsPRMT6a-FLAG*. The plasmids were then transiently expressed in *N*. *benthamiana* leaves via *Agrobacterium*-mediated transfection or in rice protoplasts.

Total protein extracts from *p35S*:*OsJAZ1-GFP*/WT and *p35S*:*OsJAZ1-GFP*/*osprmt6a-1* transgenic rice plants were prepared for the cell-free *in vivo* Co-IP assay. Magnetic anti-GFP monoclonal antibody (mAb) beads (D153-11, Medical Biological Laboratories) were used for immunoprecipitation of OsJAZ1-GFP fusion proteins, which resulted in enrichment of native OsCOI1a proteins or MBP-OsCOI1b fusion proteins.

The detailed methods used for protein extraction and immunoprecipitation have been described previously (Zhou et al., 2013). Proteins were subsequently separated on 10% SDS–PAGE gels and detected by western blotting with an anti-GFP antibody (598-7, Medical Biological Laboratories, 1:5000), an anti-FLAG antibody (M185-7, Medical Biological Laboratories, 1:5000), and an anti-OsCOI1a antibody (AbP80385-A-SE, Beijing Protein Innovation, 1:1000).

Prokaryotic protein expression

To generate MBP and His-tag fusion proteins, the full-length CDSs of *OsJAZ1*, *OsJAZ1* (*1K*), *OsJAZ1* (*5K*), *OsJAZ7*, *OsMYC2*, and *OsCOI1b* were amplified, cloned, and inserted into the pMalc2x vector. The OsJAZ1 (1K) and OsJAZ1 (5K) proteins were mimics of demethylated OsJAZ1 protein. The coding sequences of *OsJAZ1* (*1K*) and *OsJAZ1* (*5K*) were generated via base substitution as described above. The CDS of *OsPRMT6a* was also amplified, cloned, and inserted into the pET28a vector. Subsequently, the MBP-OsJAZ1, MBP-OsJAZ1 (1K), MBP-OsJAZ1 (5K), MBP-OsJAZ7, MBP-OsCOI1b, MBP-OsMYC2, and MBP proteins were expressed in cells of *E*. *coli* strain BL21 (DE3, TransGen). Cells were induced with 0.1 mM isopropyl-β-D-thiogalactoside (IPTG) and shaken at 16°C for 18 h, and the proteins were purified using amylose resin (E8021S, New England Biolabs). The His-PRMT6a protein was expressed by induction with 1 mM IPTG, followed by shaking at 18°C for 18 h. The protein was then purified using IDA-Nickel (70 501-100, BEAVER). The detailed methods for protein purification have been described previously (Duan et al., 2019).

In vitro pull-down assay

His-OsPRMT6a was used as bait to pull down approximately equal amounts of MBP, MBP-OsJAZ1, MBP-OsJAZ1 (1K), MBP-OsJAZ1 (5K), and MBP-OsJAZ7 with amylose resin (E8021S, New England Biolabs). Anti-MBP (E8032S, New England Biolabs, 1:5000) and anti-His (D291-7, Medical Biological Laboratories, 1:5000) antibodies were used to detect the proteins. The detailed methods used for the *in vitro* pull-down assay have been described previously (Zhou et al., 2013).

Luciferase complementation imaging assay

The CDS of *OsPRMT6a* was fused to pCAMBIA1300-nLUC, and the CDSs of *OsJAZ1*, *OsJAZ7*, *OsJAZ8*, and *OsCOI1a* were fused to pCAMBIA1300-cLUC vectors. The empty vectors pCAMBIA1300-nLUC and pCAMBIA1300-cLUC were used as negative controls. The plasmids were transiently coexpressed in *N*. *benthamiana* leaves via *Agrobacterium*-mediated transfection. The injected leaves were sprayed with 10 mM beetle luciferin (Promega, E1602) and placed in darkness for 3 min before luminescence detection. LUC images were then captured with a charge-coupled device imaging apparatus (Berthold, LB985).

Bimolecular fluorescence complementation assay

The CDS of *OsJAZ1* was fused to YNE of the p2YN vector. The CDSs of *OsCOI1a* and *OsPRMT6a* were fused to YCE of the p2YC vector. The plasmids were transiently coexpressed in *N*. *benthamiana* leaves via *Agrobacterium*-mediated transfection. Fluorescence signals were detected using a confocal microscope (Zeiss LSM 880). The detailed methods have been described previously (Waadt and Kudla, 2008).

In vitro methylation assay

The prokaryotically expressed protein His-OsPRMT6a was incubated separately with MBP-OsJAZ1, MBP-OsJAZ1 (1K), and MBP-OsJAZ1 (5K) for 4 h at 4°C in a reaction mixture containing MTS buffer (20 mM Tris [pH 7.5], 200 mM NaCl, 0.4 mM EDTA). The proteins were then separated by 10% SDS–PAGE and detected by western blotting with anti-methylarginine antibodies (#8015, #13222, #13522; Cell Signaling Technology, 1:1000). The protein OsJAZ1 modified by arginine methylation, which was obtained through an *in vitro* methylation assay, was also subjected to mass spectrometry analysis. The details of the methods have been described previously (Lucher and Lego, 1989; Blifernez et al., 2011).

In vivo methylation assay

Fifteen-day-old rice seedlings of the *p35S*:*OsJAZ1-GFP*/WT and *p35S*:*OsJAZ1-GFP*/*osprmt6a-1* transgenic lines were frozen in liquid nitrogen and ground to powder. Total protein was extracted from fresh powder in triple volumes of NB1 buffer (50 mM Tris–2-(*N-morpholino)ethanesulfonic acid [*MES] [pH 8.0], 1 mM $MgCl_2$, 0.5 M sucrose, 10 mM EDTA, and 5 mM dithiothreitol [DTT]) containing a proteinase inhibitor cocktail (Roche, 04693132001). The denatured proteins (95°C, 5 min) were then separated on 10% SDS–PAGE gels and detected by western blotting with anti-methylarginine antibodies (#8015, #13222, #13522; Cell Signaling Technology, 1:1000), with anti-OsJAZ1 (ABclonal, 1:1000) and anti-HSP82 antibodies (AbM51099–31-PU; Beijing Protein Innovation, 1:5000) used as loading controls.

In vivo degradation assay

Fifteen-day-old WT, *osprmt6a-1*, *p35S*:*OsJAZ1-GFP*/WT, *p35S*:*OsJAZ1-GFP*/*osprmt6a-1*, and *pCAMBIA1390-OsPRMT6a-FLAG* transgenic rice seedlings were treated with a specific concentration of MeJA, then collected at specific time points. To prevent protein degradation, the seedlings were pretreated with

40 μM MG132 (Calbiochem) for 3 h. Details of subsequent experimental procedures were as described above (Zhou et al., 2013).

Analysis of OsJAZ1-GFP and arginine methylation levels during rice spikelet development

We collected rice spikelets in the field in Shunyi district (Beijing) from the tillering stage and booting stage to the heading stage and stored them in liquid nitrogen. The collected spikelets were divided into different developmental stages according to inflorescence length and morphology as defined by Ikeda et al. (2004): In 3–5 (In 3, ≤0.9-mm-long inflorescence with hairs, primary branch formation, 0.2–0.4 mm long; In 4, elongation of primary branches, 0.4- to 0.6-mm-long inflorescence; In 5, formation of high-order branches, 0.6- to 0.9-mm-long inflorescence); In 6 (differentiation of glumes, 0.9- to 1.5-mm-long inflorescence with looming spikelet); In 7 (differentiation of floral organs, 1.5- to 40-mm-long inflorescence with clearly visible spikelet); In 8 (rapid elongation of rachis and branches, 40- to 220-mm-long inflorescence); and In 9 (heading and flowering, ≥220-mm-long inflorescence).

For western blotting analysis, we used HSP82 as the internal control to ensure consistent protein loading across different samples. "OsJAZ1-GFP/HSP82" represents the relative OsJAZ1-GFP content per unit of spikelet fresh weight. "Methyl/(OsJAZ1-GFP/HSP82)" represents the relative arginine methylation level per unit of OsJAZ1-GFP. HSP82 was used as an internal control to quantify the relative protein content of OsJAZ1-GFP in different samples so that the relative arginine methylation levels between different samples could be compared.

In vivo dual-luciferase degradation assay

To investigate differences in degradation levels of OsJAZ1 and OsJAZ1 (5K), the 651-bp CDS (excluding the stop codon) of *OsJAZ1*/*OsJAZ1* (*5K*) under the control of the CaMV35S promoter was inserted into the *Nco*I restriction site upstream of LUC in the pGreenII 0800-LUC transient expression vector to construct *p35S*:*OsJAZ1-LUC* and *p35S*:*OsJAZ1* (*5K*)*-LUC*. The plasmids for these constructs were transiently expressed in *N. benthamiana* leaves via *Agrobacterium*-mediated transfection. Leaf samples were collected at 48 h and 72 h post infection. The collected fresh tissue was frozen in liquid nitrogen and ground to powder. Total protein was extracted from freshly harvested leaves in triple volumes of NB1 buffer (50 mM Tris–MES, [pH 8.0], 1 mM $MgCl_2$, 0.5 M sucrose. 10 mM EDTA. 5 mM DTT) containing a proteinase inhibitor cocktail (Roche, 04693132001). LUC activity was measured using the Dual-LUC Reporter Assay System (Promega, E2920). The Dual-Glo Luciferase Assay System (Promega) was used for measuring LUC activity.

Cell-free degradation assay

Fresh tissues from 15-day-old *p35S*:*OsJAZ1-GFP*/WT and *p35S*:*OsJAZ1-GFP*/*osprmt6a-1* transgenic plants were ground and pulverized to extract total protein in degradation buffer (Wang et al., 2009; Lin et al., 2012). The *E. coli*–expressed fusion proteins MBP-OsJAZ1 and MBP-OsJAZ1 (5K) were separately added to the total plant proteins, and the mixture was sampled at 0, 0.5, and 1 h. Subsequently, MG132 (Calbiochem) was selectively added for various *in vitro* degradation assays as indicated. Denatured proteins (95°C, 5 min) were separated by 10% SDS–PAGE and detected by western blotting with an anti-MBP antibody. The methods used have been described previously (Lin et al., 2012).

Semi-*in vivo* Co-IP assay

Total protein extracts were prepared from the *p35S*:*OsJAZ1-GFP*/WT and *p35S*:*OsJAZ1-GFP*/*osprmt6a-1* transgenic plants as described for the cell-free degradation assay. Purified MBP-OsCOI1b fusion proteins (approximately 1 μg) were fixed to anti-GFP mAb magnetic beads and incubated in 400 μl of plant extract in the presence of a protease inhibitor cocktail (Roche). The mixture was gently shaken at 28°C for 30 min. The subsequent steps mirrored those of the *in vivo* Co-IP assay. Western blotting analysis was performed using anti-MBP or anti-GFP antibodies. The methods used have been described previously (Lin et al., 2012).

In vitro ubiquitination assay

Purified MBP-OsJAZ1 protein bound to amylose resin (NEB) was incubated at 28°C with equal amounts of rice seedling crude extract in binding buffer. The details of the methods used have been described previously (Lin et al., 2012). The supernatants containing OsJAZ1 or OsJAZ1-(Ub)n were then separated by 10% SDS–PAGE and detected by western blotting with an anti-MBP antibody.

RNA-seq analysis

Total RNA was extracted from approximately 1-cm-long inflorescences, and RNA quality (integrity) was assessed using an Agilent 2100 Bioanalyzer. Only RNA samples with an RNA integrity number greater than 7 were used for subsequent analyses.

After sample quality assessment, mRNA was enriched using magnetic beads with oligo(dT) sequences, which bind to the poly(A) tail of mRNA through A–T complementary pairing. The mRNA was fragmented using fragmentation buffer, and first-strand cDNA was synthesized using random hexamers as primers. Double-stranded cDNA was generated by addition of a buffer, deoxynucleotide triphosphates, and DNA polymerase I and was then purified using AMPure XP beads. The purified double-stranded cDNA was subjected to end repair, A-tailing, and sequencing adapter ligation. Size selection was performed using AMPure XP beads, followed by PCR enrichment to construct the final cDNA library.

After library construction, the initial quantification was performed using a Qubit 2.0 instrument. The library was diluted to 1 ng/μl, and the insert size was assessed using an Agilent 2100 instrument to ensure that it met the expected size range. The library's effective concentration was accurately quantified using qPCR to guarantee that the concentration exceeded 2 nM, thus ensuring library quality. Once the libraries were subjected to quality control, different libraries were pooled on the basis of their effective concentrations and the desired target data volume.

The raw sequencing data were preprocessed to remove adapter sequences and low-quality bases using Trimmomatic. Cleaned reads were aligned to the *O. sativa* reference genome (RAP, The Rice Annotation Project). Gene expression levels were quantified using StringTie, and differential gene expression analysis was performed with DESeq2. Functional annotation and pathway

analysis of differentially expressed genes were performed using the Gene Ontology and Kyoto Encyclopedia of Genes and Genomes (KEGG) databases.

Electrophoretic mobility shift assay

Biotin-labeled DNA probes were synthesized by Invitrogen. A Light-Shift Chemiluminescent EMSA Kit (Thermo Fisher, 20148) was used according to the manufacturer's instructions. Details of the methods used have been described previously (Duan et al., 2019).

Yeast one-hybrid assay

The full-length CDS of *OsMYC2* was cloned and inserted into the pB42AD vector at the *Eco*RI restriction site to obtain the *pB42AD-OsMYC2* construct. To investigate promoter activity, the full 2.2-kb region and various truncated versions of the *OsPRMT6a* promoter were amplified using primers and inserted into the *Xho*I restriction site of the pLacZi reporter vector. The resulting constructs were cotransformed into the yeast strain EGY48. The empty pB42AD vector combined with the *LacZ* reporter construct was used as a negative control. The details of the methods used have been described previously (Duan et al., 2019).

Dual-luciferase transient reporter gene assay

The 2.2-kb promoter region of *OsPRMT6a* was amplified, cloned, and inserted into the pGreenII 0800-LUC vector (Zhou et al., 2013) to generate the *pGreenII 0800-pro6A-LUC* reporter construct. The full-length CDS of *OsMYC2* was amplified, cloned, and inserted into the pCAMBIA1305-GFP vector to generate the *p35S*:*OsMYC2-GFP* effector construct, and the empty pCAMBIA1305-GFP vector was used as the negative control. The plasmids were transiently expressed in *N. benthamiana* leaves via *Agrobacterium*-mediated transfection. LUC and REN activities were analyzed using a dual-luciferase reporter kit following the manufacturer's instructions (Promega). The absolute LUC/REN ratio was measured in a TriStar Multimode Reader LB 942 (Berthold Technologies).

Chromatin immunoprecipitation assay

The *OsPRMT6a* promoter and full-length sequence, spanning 6.8 kb, were amplified and inserted into the *NcoI* restriction site upstream of LUC in the pGreenII 0800-LUC transient expression vector (Zhou et al., 2013) to generate the *pGreenII 0800-6A-LUC* reporter construct. The *pGreenII 0800-6A-LUC* and *p35S*:*OsMYC2-GFP* plasmids were cotransfected into young tobacco leaves. The solubilized chromatin was then immunoprecipitated using an anti-GFP antibody or rabbit immunoglobulin G (#2729, Cell Signaling Technology) at 4°C for 8 h. After immunoprecipitation, DNA was collected using Magna ChIP protein A magnetic beads (16-661, EMD Millipede). For each ChIP–qPCR, the DNA recovered from the immunoprecipitate was used as a template. The detailed methods have been described previously (Li et al., 2011).

DATA AND CODE AVAILABILITY

The raw RNA-seq data reported in this paper have been deposited at the Genome Sequence Archive (Chen et al., 2021) of the National Genomics Data Center (CNCB-NGDC members and partners, 2022), China National Center for Bioinformation/Beijing Institute of Genomics, Chinese Academy of Sciences (GSA: CRA016196), and are publicly accessible at https://ngdc.cncb.ac.cn/gsa and at the NCBI Sequence Read Archive under accession number NCBI: PRJNA1034168.

SUPPLEMENTAL INFORMATION

Supplemental information is available at *Molecular Plant Online*.

FUNDING

We thank Prof. Qiang Cai (College of Life Sciences, Wuhan University) and Prof. Zheng Yuan (School of Life Sciences and Biotechnology, Shanghai Jiao Tong University) for providing morphology data for the *eg1-1* and *eg2-1D* mutants. This work was supported by grants from the National Key R&D Program of China (2022YFD1200100), STI 2030 - Major Projects (2023ZD0406802), and the National Natural Science Foundation of China (no. 92035301 and no. 31771765).

AUTHOR CONTRIBUTIONS

J.W., Q.L., and Z.C. supervised the project. K.D. designed the research. K.D., Q.L., and C.W. wrote the paper. F.W. provided the plant material. K.D. performed most of the experiments. K.D. and S.C. analyzed the data. S.C. performed the cytological observations. S. Li performed the Y1H assay, LUC transient reporter gene assay, and ChIP assay; M.F. performed RNA *in situ* hybridization. R.M. performed the subcellular localization assay. C.W., Q.L., F.W., F.Z., S.L., X.Y., X.Z., C.L., Y.R., and S.Z. provided technical assistance. S.C., X.J., X.X., and Y.C. performed a portion of the RT–qPCR analysis. X.G. and D.Y. generated the transgenic plants. K.D., S.C., P.W., and S.Z. cultivated the transgenic plants in the field.

ACKNOWLEDGMENTS

The authors declare no competing interests.

Received: December 7, 2023
Revised: April 4, 2024
Accepted: April 29, 2024
Published: May 4, 2024

REFERENCES

Acosta, I.F., Laparra, H., Romero, S.P., Schmelz, E., Hamberg, M., Mottinger, J.P., Moreno, M.A., and Dellaporta, S.L. (2009). *tasselseed1* is a lipoxygenase affecting jasmonic acid signaling in sex determination of maize. Science **323**:262–265.

Ahmad, A., Dong, Y., and Cao, X. (2011). Characterization of the *PRMT* gene family in rice reveals conservation of arginine methylation. PLoS One **6:**e22664.

Bedford, M.T., and Clarke, S.G. (2009). Protein arginine methylation in mammals: who, what, and why. Mol. Cell **33**:1–13.

Blanc, R.S., and Richard, S. (2017). Arginine methylation: the coming of age. Mol. Cell **65**:8–24.

Blifernez, O., Wobbe, L., Niehaus, K., and Kruse, O. (2011). Protein arginine methylation modulates light-harvesting antenna translation in *Chlamydomonas reinhardtii*. Plant J. **65**:119–130.

Brown, R.L., Kazan, K., McGrath, K.C., Maclean, D.J., and Manners, J.M. (2003). A role for the GCC-box in jasmonate-mediated activation of the *PDF1.2* gene of *Arabidopsis*. Plant Physiol. **132**:1020–1032.

Browse, J., and Howe, G.A. (2008). New weapons and a rapid response against insect attack. Plant Physiol. **146**:832–838.

Cai, Q., Yuan, Z., Chen, M., Yin, C., Luo, Z., Zhao, X., Liang, W., Hu, J., and Zhang, D. (2014). Jasmonic acid regulates spikelet development in rice. Nat. Commun. **5**:3476.

Cao, L., Tian, J., Liu, Y., Chen, X., Li, S., Persson, S., Lu, D., Chen, M., Luo, Z., Zhang, D., and Yuan, Z. (2021). Ectopic expression of OsJAZ6, which interacts with OsJAZ1, alters JA signaling and spikelet development in rice. Plant J. **108**:1083–1096.

Carr, S.M., Munro, S., Kessler, B., Oppermann, U., and La Thangue, N.B. (2011). Interplay between lysine methylation and Cdk phosphorylation in growth control by the retinoblastoma protein. EMBO J. **30**:317–327.

Chen, T., Chen, X., Zhang, S., Zhu, J., Tang, B., Wang, A., Dong, L., Zhang, Z., Yu, C., Sun, Y., et al. (2021). The Genome Sequence Archive family: toward explosive data growth and diverse data types. Dev. Reprod. Biol. **19**:578–583.

Chen, Z.X., Wu, J.G., Ding, W.N., Chen, H.M., Wu, P., and Shi, C.H. (2006). Morphogenesis and molecular basis on naked seed rice, a novel homeotic mutation of *OsMADS1* regulating transcript level of *AP3* homologue in rice. Planta **223**:882–890.

Cheng, X., Collins, R.E., and Zhang, X. (2005). Structural and sequence motifs of protein (histone) methylation enzymes. Annu. Rev. Biophys. Biomol. Struct. **34**:267–294.

Cheong, Y.H., Chang, H.S., Gupta, R., Wang, X., Zhu, T., and Luan, S. (2002). Transcriptional profiling reveals novel interactions between wounding, pathogen, abiotic stress, and hormonal responses in *Arabidopsis*. Plant Physiol. **129**:661–677.

Chico, J.M., Lechner, E., Fernandez-Barbero, G., Canibano, E., García-Casado, G., Franco-Zorrilla, J.M., Hammann, P., Zamarreño, A.M., García-Mina, J.M., Rubio, V., et al. (2020). CUL3^{BPM} E3 ubiquitin ligases regulate MYC2, MYC3, and MYC4 stability and JA responses. Proc. Natl. Acad. Sci. USA **117**:6205–6215.

Chini, A., Fonseca, S., Fernández, G., Adie, B., Chico, J.M., Lorenzo, O., García-Casado, G., López-Vidriero, I., Lozano, F.M., Ponce, M.R., et al. (2007). The JAZ family of repressors is the missing link in jasmonate signalling. Nature **448**:666–671.

Chung, H.S., and Howe, G.A. (2009). A critical role for the TIFY motif in repression of jasmonate signaling by a stabilized splice variant of the JASMONATE ZIM-domain protein JAZ10 in *Arabidopsis*. Plant Cell **21**:131–145.

Cui, R., Han, J., Zhao, S., Su, K., Wu, F., Du, X., Xu, Q., Chong, K., Theissen, G., and Meng, Z. (2010). Functional conservation and diversification of class E floral homeotic genes in rice (*Oryza sativa*). Plant J. **61**:767–781.

CNCB-NGDC Members and Partners. (2022). Database resources of the National Genomics Data Center, China National Center for Bioinformation in 2022. Nucleic Acids Res. **50:**D27-d38.

Devoto, A., Nieto-Rostro, M., Xie, D., Ellis, C., Harmston, R., Patrick, E., Davis, J., Sherratt, L., Coleman, M., and Turner, J.G. (2002). COI1 links jasmonate signalling and fertility to the SCF ubiquitin-ligase complex in *Arabidopsis*. Plant J. **32**:457–466.

Dombrecht, B., Xue, G.P., Sprague, S.J., Kirkegaard, J.A., Ross, J.J., Reid, J.B., Fitt, G.P., Sewelam, N., Schenk, P.M., Manners, J.M., and Kazan, K. (2007). MYC2 differentially modulates diverse jasmonate-dependent functions in *Arabidopsis*. Plant Cell **19**:2225–2245.

Duan, E., Wang, Y., Li, X., Lin, Q., Zhang, T., Wang, Y., Zhou, C., Zhang, H., Jiang, L., Wang, J., et al. (2019). OsSHI1 regulates plant architecture through modulating the transcriptional activity of IPA1 in rice. Plant Cell **31**:1026–1042.

Estève, P.O., Chang, Y., Samaranayake, M., Upadhyay, A.K., Horton, J.R., Feehery, G.R., Cheng, X., and Pradhan, S. (2011). A methylation and phosphorylation switch between an adjacent lysine and serine determines human DNMT1 stability. Nat. Struct. Mol. Biol. **18**:42–48.

Fang, L., Zhang, L., Wei, W., Jin, X., Wang, P., Tong, Y., Li, J., Du, J.X., and Wong, J. (2014). A methylation-phosphorylation switch determines Sox2 stability and function in ESC maintenance or differentiation. Mol. Cell **55**:537–551.

Feng, X., Zhang, L., Wei, X., Zhou, Y., Dai, Y., and Zhu, Z. (2020). OsJAZ13 negatively regulates jasmonate signaling and activates hypersensitive cell death response in rice. Int. J. Mol. Sci. **21:**4379.

Goossens, J., Mertens, J., and Goossens, A. (2017). Role and functioning of bHLH transcription factors in jasmonate signalling. J. Exp. Bot. **68**:1333–1347.

Guo, Q., Yoshida, Y., Major, I.T., Wang, K., Sugimoto, K., Kapali, G., Havko, N.E., Benning, C., and Howe, G.A. (2018). JAZ repressors of metabolic defense promote growth and reproductive fitness in *Arabidopsis*. Proc. Natl. Acad. Sci. USA **115**:E10768–E10777.

Hang, R., Liu, C., Ahmad, A., Zhang, Y., Lu, F., and Cao, X. (2014). *Arabidopsis* protein arginine methyltransferase 3 is required for ribosome biogenesis by affecting precursor ribosomal RNA processing. Proc. Natl. Acad. Sci. USA **111**:16190–16195.

He, Y., Hong, G., Zhang, H., Tan, X., Li, L., Kong, Y., Sang, T., Xie, K., Wei, J., Li, J., et al. (2020). The OsGSK2 kinase integrates brassinosteroid and jasmonic acid signaling by interacting with OsJAZ4. Plant Cell **32**:2806–2822.

Hiei, Y., Ohta, S., Komari, T., and Kumashiro, T. (1994). Efficient transformation of rice (*Oryza sativa L.*) mediated by *Agrobacterium* and sequence analysis of the boundaries of the T-DNA. Plant J. **6**:271–282.

Hong, S., Song, H.R., Lutz, K., Kerstetter, R.A., Michael, T.P., and McClung, C.R. (2010). Type II protein arginine methyltransferase 5 (PRMT5) is required for circadian period determination in *Arabidopsis thaliana*. Proc. Natl. Acad. Sci. USA **107**:21211–21216.

Hori, Y., Kurotani, K.I., Toda, Y., Hattori, T., and Takeda, S. (2014). Overexpression of the JAZ factors with mutated jas domains causes pleiotropic defects in rice spikelet development. Plant Signal. Behav. **9**:e970414.

Hu, S., Yu, K., Yan, J., Shan, X., and Xie, D. (2023). Jasmonate perception: Ligand-receptor interaction, regulation, and evolution. Mol. Plant **16**:23–42.

Huang, H., Liu, B., Liu, L., and Song, S. (2017). Jasmonate action in plant growth and development. J. Exp. Bot. **68**:1349–1359.

Ikeda, K., Sunohara, H., and Nagato, Y. (2004). Developmental course of inflorescence and spikelet in rice. Breed Sci. **54**:147–156.

Ivanov, G.S., Ivanova, T., Kurash, J., Ivanov, A., Chuikov, S., Gizatullin, F., Herrera-Medina, E.M., Rauscher, F., 3rd, Reinberg, D., and Barlev, N.A. (2007). Methylation-acetylation interplay activates p53 in response to DNA damage. Mol. Cell Biol. **27**:6756–6769.

Jeon, J.S., Jang, S., Lee, S., Nam, J., Kim, C., Lee, S.H., Chung, Y.Y., Kim, S.R., Lee, Y.H., Cho, Y.G., and An, G. (2000). *leafy hull sterile1* is a homeotic mutation in a rice MADS box gene affecting rice flower development. Plant Cell **12**:871–884.

Katsir, L., Schilmiller, A.L., Staswick, P.E., He, S.Y., and Howe, G.A. (2008). COI1 is a critical component of a receptor for jasmonate and the bacterial virulence factor coronatine. Proc. Natl. Acad. Sci. USA **105**:7100–7105.

Kim, E.H., Kim, Y.S., Park, S.H., Koo, Y.J., Choi, Y.D., Chung, Y.Y., Lee, I.J., and Kim, J.K. (2009). Methyl jasmonate reduces grain yield by mediating stress signals to alter spikelet development in rice. Plant Physiol. **149**:1751–1760.

Komatsu, M., Chujo, A., Nagato, Y., Shimamoto, K., and Kyozuka, J. (2003). *FRIZZY PANICLE* is required to prevent the formation of axillary meristems and to establish floral meristem identity in rice spikelets. Development **130**:3841–3850.

Lee, D.Y., and An, G. (2012). Two AP2 family genes, *supernumerary bract* (*SNB*) and *Osindeterminate spikelet 1* (*OsIDS1*), synergistically control

inflorescence architecture and floral meristem establishment in rice. Plant J. **69**:445–461.

Lee, D.Y., Lee, J., Moon, S., Park, S.Y., and An, G. (2007). The rice heterochronic gene *SUPERNUMERARY BRACT* regulates the transition from spikelet meristem to floral meristem. Plant J. **49**:64–78.

Lee, H.Y., Seo, J.S., Cho, J.H., Jung, H., Kim, J.K., Lee, J.S., Rhee, S., and Do Choi, Y. (2013). *Oryza sativa COI* homologues restore jasmonate signal transduction in *Arabidopsis coi1-1* mutants. PLoS One **8:**e52802.

Lei, Y., Lu, L., Liu, H.Y., Li, S., Xing, F., and Chen, L.L. (2014). CRISPR-P: a web tool for synthetic single-guide RNA design of CRISPR-system in plants. Mol. Plant **7**:1494–1496.

Lescot, M., Déhais, P., Thijs, G., Marchal, K., Moreau, Y., Van de Peer, Y., Rouzé, P., and Rombauts, S. (2002). PlantCARE, a database of plant cis-acting regulatory elements and a portal to tools for *in silico* analysis of promoter sequences. Nucleic Acids Res. **30**:325–327.

Li, H., Xue, D., Gao, Z., Yan, M., Xu, W., Xing, Z., Huang, D., Qian, Q., and Xue, Y. (2009). A putative lipase gene *EXTRA GLUME1* regulates both empty-glume fate and spikelet development in rice. Plant J. **57**:593–605.

Li, H., Liang, W., Hu, Y., Zhu, L., Yin, C., Xu, J., Dreni, L., Kater, M.M., and Zhang, D. (2011). Rice *MADS6* interacts with the floral homeotic genes *SUPERWOMAN1*, *MADS3*, *MADS58*, *MADS13*, and *DROOPING LEAF* in specifying floral organ identities and meristem fate. Plant Cell **23**:2536–2552.

Lim, J., Moon, Y.H., An, G., and Jang, S.K. (2000). Two rice MADS domain proteins interact with *OsMADS1*. Plant Mol. Biol. **44**:513–527.

Lin, Q., Wang, D., Dong, H., Gu, S., Cheng, Z., Gong, J., Qin, R., Jiang, L., Li, G., Wang, J.L., et al. (2012). Rice APC/C^{TE} controls tillering by mediating the degradation of MONOCULM 1. Nat. Commun. **3**:752.

Lorenzo, O., Chico, J.M., Sánchez-Serrano, J.J., and Solano, R. (2004). *JASMONATE-INSENSITIVE1* encodes a MYC transcription factor essential to discriminate between different jasmonate-regulated defense responses in *Arabidopsis*. Plant Cell **16**:1938–1950.

Lucher, L.A., and Lego, T. (1989). Use of the water-soluble fluor sodium salicylate for fluorographic detection of tritium in thin-layer chromatograms and nitrocellulose blots. Anal. Biochem. **178**:327–330.

Malcomber, S.T., and Kellogg, E.A. (2004). Heterogeneous expression patterns and separate roles of the *SEPALLATA* gene *LEAFY HULL STERILE1* in grasses. Plant Cell **16**:1692–1706.

Mou, Z., He, Y., Dai, Y., Liu, X., and Li, J. (2000). Deficiency in fatty acid synthase leads to premature cell death and dramatic alterations in plant morphology. Plant Cell **12**:405–418.

Pauwels, L., Morreel, K., De Witte, E., Lammertyn, F., Van Montagu, M., Boerjan, W., Inzé, D., and Goossens, A. (2008). Mapping methyl jasmonate-mediated transcriptional reprogramming of metabolism and cell cycle progression in cultured *Arabidopsis* cells. Proc. Natl. Acad. Sci. USA **105**:1380–1385.

Pei, Y., Niu, L., Lu, F., Liu, C., Zhai, J., Kong, X., and Cao, X. (2007). Mutations in the Type II protein arginine methyltransferase AtPRMT5 result in pleiotropic developmental defects in *Arabidopsis*. Plant Physiol. **144**:1913–1923.

Ren, D., Li, Y., Zhao, F., Sang, X., Shi, J., Wang, N., Guo, S., Ling, Y., Zhang, C., Yang, Z., and He, G. (2013). MULTI-FLORET SPIKELET1, which encodes an AP2/ERF protein, determines spikelet meristem fate and sterile lemma identity in rice. Plant Physiol. **162**:872–884.

Reymond, P., Weber, H., Damond, M., and Farmer, E.E. (2000). Differential gene expression in response to mechanical wounding and insect feeding in *Arabidopsis*. Plant Cell **12**:707–720.

Scebba, F., De Bastiani, M., Bernacchia, G., Andreucci, A., Galli, A., and Pitto, L. (2007). PRMT11: a new *Arabidopsis* MBD7 protein partner with arginine methyltransferase activity. Plant J. **52**:210–222.

Schmitz, R.J., Sung, S., and Amasino, R.M. (2008). Histone arginine methylation is required for vernalization-induced epigenetic silencing of *FLC* in winter-annual *Arabidopsis thaliana*. Proc. Natl. Acad. Sci. USA **105**:411–416.

Sheard, L.B., Tan, X., Mao, H., Withers, J., Ben-Nissan, G., Hinds, T.R., Kobayashi, Y., Hsu, F.F., Sharon, M., Browse, J., et al. (2010). Jasmonate perception by inositol-phosphate-potentiated COI1-JAZ co-receptor. Nature **468**:400–405.

Taylor, S.C., Berkelman, T., Yadav, G., and Hammond, M. (2013). A defined methodology for reliable quantification of Western blot data. Mol. Biol. **55**:217–226.

Thines, B., Parlan, E.V., and Fulton, E.C. (2019). Circadian network interactions with jasmonate signaling and defense. Plants-Basel **8**:252.

Thines, B., Katsir, L., Melotto, M., Niu, Y., Mandaokar, A., Liu, G., Nomura, K., He, S.Y., Howe, G.A., and Browse, J. (2007). JAZ repressor proteins are targets of the SCF^{COI1} complex during jasmonate signalling. Nature **448**:661–665.

Tong, H., Jin, Y., Liu, W., Li, F., Fang, J., Yin, Y., Qian, Q., Zhu, L., and Chu, C. (2009). DWARF AND LOW-TILLERING, a new member of the GRAS family, plays positive roles in brassinosteroid signaling in rice. Plant J. **58**:803–816.

Waadt, R., and Kudla, J. (2008). planta visualization of protein interactions using bimolecular fluorescence complementation (BiFC). CSH Protoc **2008**, pdb.prot4995.

Wang, F., Zhu, D., Huang, X., Li, S., Gong, Y., Yao, Q., Fu, X., Fan, L.M., and Deng, X.W. (2009). Biochemical insights on degradation of *Arabidopsis* DELLA proteins gained from a cell-free assay system. Plant Cell **21**:2378–2390.

Wang, X., Zhang, Y., Ma, Q., Zhang, Z., Xue, Y., Bao, S., and Chong, K. (2007). SKB1-mediated symmetric dimethylation of histone H4R3 controls flowering time in *Arabidopsis*. EMBO J. **26**:1934–1941.

Wolf, S.S. (2009). The protein arginine methyltransferase family: an update about function, new perspectives and the physiological role in humans. Cell. Mol. Life Sci. **66**:2109–2121.

Wolters, H., and Jürgens, G. (2009). Survival of the flexible: hormonal growth control and adaptation in plant development. Nat. Rev. Genet. **10**:305–317.

Wu, H., Ye, H., Yao, R., Zhang, T., and Xiong, L. (2015). OsJAZ9 acts as a transcriptional regulator in jasmonate signaling and modulates salt stress tolerance in rice. Plant Sci. **232**:1–12.

Wu, Y., Wang, Y., Mi, X.F., Shan, J.X., Li, X.M., Xu, J.L., and Lin, H.X. (2016). The QTL *GNP1* encodes GA20ox1, which increases grain number and yield by increasing cytokinin activity in rice panicle meristems. PLoS Genet. **12:**e1006386.

Xu, L., Liu, F., Lechner, E., Genschik, P., Crosby, W.L., Ma, H., Peng, W., Huang, D., and Xie, D. (2002). The SCF^{COI1} ubiquitin-ligase complexes are required for jasmonate response in *Arabidopsis*. Plant Cell **14**:1919–1935.

Yamada, S., Kano, A., Tamaoki, D., Miyamoto, A., Shishido, H., Miyoshi, S., Taniguchi, S., Akimitsu, K., and Gomi, K. (2012). Involvement of OsJAZ8 in jasmonate-induced resistance to bacterial blight in rice. Plant Cell Physiol. **53**:2060–2072.

Yamagata, K., Daitoku, H., Takahashi, Y., Namiki, K., Hisatake, K., Kako, K., Mukai, H., Kasuya, Y., and Fukamizu, A. (2008). Arginine methylation of FOXO transcription factors inhibits their phosphorylation by Akt. Mol. Cell **32**:221–231.

Yan, D., Zhang, Y., Niu, L., Yuan, Y., and Cao, X. (2007). Identification and characterization of two closely related histone H4 arginine 3 methyltransferases in *Arabidopsis thaliana*. Biochem. J. **408**:113–121.

Yan, H., Yoo, M.J., Koh, J., Liu, L., Chen, Y., Acikgoz, D., Wang, Q., and Chen, S. (2014). Molecular reprogramming of *Arabidopsis* in response to perturbation of jasmonate signaling. J. Proteome Res. **13**:5751–5766.

Yang, D.-L., Yao, J., Mei, C.-S., Tong, X.-H., Zeng, L.-J., Li, Q., Xiao, L.-T., Sun, T.-p., Li, J., Deng, X.-W., et al. (2012). Plant hormone jasmonate prioritizes defense over growth by interfering with gibberellin signaling cascade. Proc. Natl. Acad. Sci. USA **109**:E1192–E1200.

Yang, J., Huang, J., Dasgupta, M., Sears, N., Miyagi, M., Wang, B., Chance, M.R., Chen, X., Du, Y., Wang, Y., et al. (2010). Reversible methylation of promoter-bound STAT3 by histone-modifying enzymes. Proc. Natl. Acad. Sci. USA **107**:21499–21504.

Ye, H., Du, H., Tang, N., Li, X., and Xiong, L. (2009). Identification and expression profiling analysis of *TIFY* family genes involved in stress and phytohormone responses in rice. Plant Mol. Biol. **71**:291–305.

Yoshida, A., Suzaki, T., Tanaka, W., and Hirano, H.Y. (2009a). The homeotic gene *long sterile lemma* (*G1*) specifies sterile lemma identity in the rice spikelet. Proc. Natl. Acad. Sci. USA **106**:20103–20108.

Yoshida, H., and Nagato, Y. (2011). Flower development in rice. J. Exp. Bot. **62**:4719–4730.

Yoshida, Y., Sano, R., Wada, T., Takabayashi, J., and Okada, K. (2009b). Jasmonic acid control of GLABRA3 links inducible defense and trichome patterning in *Arabidopsis*. Development **136**:1039–1048.

You, X., Zhu, S., Zhang, W., Zhang, J., Wang, C., Jing, R., Chen, W., Wu, H., Cai, Y., Feng, Z., et al. (2019). OsPEX5 regulates rice spikelet development through modulating jasmonic acid biosynthesis. New Phytol. **224**:712–724.

Zhang, T., Li, Y., Ma, L., Sang, X., Ling, Y., Wang, Y., Yu, P., Zhuang, H., Huang, J., Wang, N., et al. (2017). *LATERAL FLORET 1* induced the three-florets spikelet in rice. Proc. Natl. Acad. Sci. USA **114**:9984–9989.

Zhang, Z., Zhang, S., Zhang, Y., Wang, X., Li, D., Li, Q., Yue, M., Li, Q., Zhang, Y.E., Xu, Y., et al. (2011). *Arabidopsis* floral initiator SKB1 confers high salt tolerance by regulating transcription and pre-mRNA splicing through altering histone H4R3 and small nuclear ribonucleoprotein LSM4 methylation. Plant Cell **23**:396–411.

Zhou, F., Lin, Q., Zhu, L., Ren, Y., Zhou, K., Shabek, N., Wu, F., Mao, H., Dong, W., Gan, L., et al. (2013). D14-SCF^{D3}-dependent degradation of D53 regulates strigolactone signalling. Nature **504**:406–410.